FINAL REPORT

on

THE USE OF A SHIP-BORNE LONG-BASELINE MICROWAVE INTERFEROMETER FOR NAVIGATION

by

MICHAEL A. MORGAN

August 1973

ONR Contract N00014-69-A-0200-1047

Space Sciences Laboratory
University of California
Berkeley, California 94720

PREFACE

Work on the development of a long base-line interferometer for wavelengths in the neighborhood of 1 cm. started in the Space Sciences and Radioastronomy Laboratories in 1970. In our annual report* for 1970-1971 we described the interferometer which we had built at the Hat Creek Radioastronomy Observatory and noted that radio sources had been located which could serve for highly accurate work on geodesy and navigation. Prof. Welch (co-principal-investigator) reported the work, early in 1972, to the annual TAC meeting for the review of the electronics program held by the Electronics Research Laboratory of the College of Engineering and at that time put forth our ideas about the use of an interferometer on board a ship as an instrument for navigation.

We then proceeded to study this matter seriously. The following report covers a rather comprehensive study carried on by Mr. Michael Morgan, a graduate student in the Dept. of Electrical Engineering and Computer Science, under the direction of Prof. Silver. The report is not only a feasibility-study but also delineates the techniques to be employed, both analytically and operationally, for locating the position of a ship on the sea from a knowledge of the position of a radio-

---

*R. Hills, W. Hoffman, M. Janssen, D.D. Thornton, S. Silver, W.J. Welch, The Development of an Interferometer for Millimeter Wavelengths, Space Sciences Laboratory Report, Series 12, Issue 64, Aug. 1971.

source in the sky.

For the wavelength region of 1 cm. a long base-line interferometer can be established on board a ship by placing the two elements -- antennas -- at the fore and aft positions of the deck; all of the lines and complex electronics can be located below deck; it is, in fact, desirable to do that. It is possible to go a step further, for, unless it is necessary to chart position continuously, the antennas can be used for other operations. One needs only a switch arrangement whereby the antennas can be connected to operate in the interferometer-mode or be disengaged from the electronics of the interferometer and tied in to other systems. The point of mentioning this is to allay arguments about costs and that the interferometer will rob the ship of other capabilities.

Whether or not the techniques developed in this report find their way into naval operations depends on the evaluation made of them by the Department of the Navy. There are undoubtedly many operational considerations to be taken into account but such matters lie outside our area of competence and responsibility. The important point is that this work stands as an example, of considerable merit in this writer's opinion, of how the pursuit of basic research, in this case in radioastronomy, can and does lead to applications and operational systems. We trust that what we are presenting in this work does have practical utility.

Samuel Silver
Principal Investigator

I. INTRODUCTION

The subject of this report is an examination of the feasibility of using a long-baseline interferometer aboard a ship as a navigational device. The ideal theoretical resolution of such an interferometer with a correlation-receiver has the potential of determining the latitude and longitude of a ship at sea with great accuracy. For example, an interferometer whose base-line is 200 meters, operating at a wavelength of 1 cm., has a central fringe of about 10 seconds of arc. By observing discrete (i.e., point-like) radio stars, whose celestial coordinates have been determined by land-based observatories, in the near zenith position relative to the ship the position of the ship on the earth can be established with an angular accuracy of about the resolving power of the interferometer. For the example quoted, a conservative estimate of this accuracy is 10 sec. of arc for the angular coordinates which represents location of position to an accuracy better than 1000 feet.

In addition to the advantage of resolving power there is the advantage that the instrument is not limited to nighttime use. As in the optical case, however, the use of the system is limited by meteorological conditions. The limitations imposed by meteorological conditions are strongly dependent on the frequency (or wavelength) at which the system operates.

The report that follows has two major subdivisions. The one deals with topics -- Preliminary Topics -- that provide the framework for computing position from certain types of data; the other deals with the special considerations of interferometry pertinent to a navigational system and the navigational technique proper.

II. PRELIMINARY TOPICS

2.1 Theory and Measurement of Ship Motions

The navigational system envisaged in this report consists of a microwave interferometer mounted on board a ship. On the ocean, the ship is a moving platform whose motions are made up of translation and rotations. The effect of such a moving platform on the operation of the interferometer is one of the major considerations in the development of the navigational system. For this reason we present, in this section, some elementary information from the theory of ship motions. A much more detailed development can be found in such references as those by Blagoreshchenskii, [1], or Beurs, [2].

A ship on the ocean is sketched in Figure 1. The cartesian axes x_1, x_2, x_3 are the body-fixed principal axes of the ship. The general motion of the vessel can be resolved into translation of the origin which is assumed to be at the center of gravity of the vessel and rotations about the principal axes. The angular displacements are shown in the figure as $\xi_1(t)$, $\xi_2(t)$, $\xi_3(t)$; in nautical circles they are known as the roll, pitch, and yaw angles, respectively. It is known from experiment, [1; pp. 338-351], that wave height on the ocean and, consequently, the roll, pitch and yaw angles have amplitudes that are random variables having Gaussian distributions. The typical sample function for any of the three random variables $\xi_i(t)$, $i = 1,2,3$, is sketched in Figure 2. The time dependence of these rotational displacements in mild and moderate sea-states is quasi-sinusoidal with an almost constant period of motion and a Gaussian distribution of

amplitudes. Typical standard deviations of roll, pitch, and yaw angles as functions of seastate for an 800 ft. vessel are given in Table 1. Some typical periods of rolling in a mild seastate for various size vessels are given in Table 2.

The geometrical factors relating the interferometer and a radio source to the principal axes are shown in Figure 3. The base-line of the interferometer is along the x_1-axis and its direction is specified by the unit vector $\hat{s}(t)$ which in a space-fixed reference system is a function of time. The radio-star-source is located by the unit vector $\hat{r}(t)$ which is a function of time in both the ship-fixed axes and the space-fixed axes by virtue of the motion of the ship and the rotation of the earth. The angle between $\hat{s}(t)$ and $\hat{r}(t)$ is denoted by $\Theta(t)$. The length of the interferometer baseline is given by $S(t)$. There will be time-dependent perturbations in this baseline length due to both the effects of mechanical stress and thermal expansion. To obtain the maximum achievable resolution of the interferometer, of the order of one "fringe width" it is necessary to know the length of the physical baseline, at all times during the operation of the system, to within a fraction of a wavelength. The variation in length due to mechanical stress will depend upon the construction of the vessel. The order of magnitude of thermal effects can be obtained by assuming that the ship is constructed of steel with a mean linear coefficient of expansion of $1.2 \times 10^{-5}\ (C°)^{-1}$. A temperature variation of 25 °C ≡ 45 °F on a vessel made of such material generates a change in length in the amount of 6 cm. in a baseline whose reference-length is 200 meters. If the wavelength of operation is 1 cm., the apparent location of sources

Figure 1 Ship Principal Axes and Rotational Displacement Angles

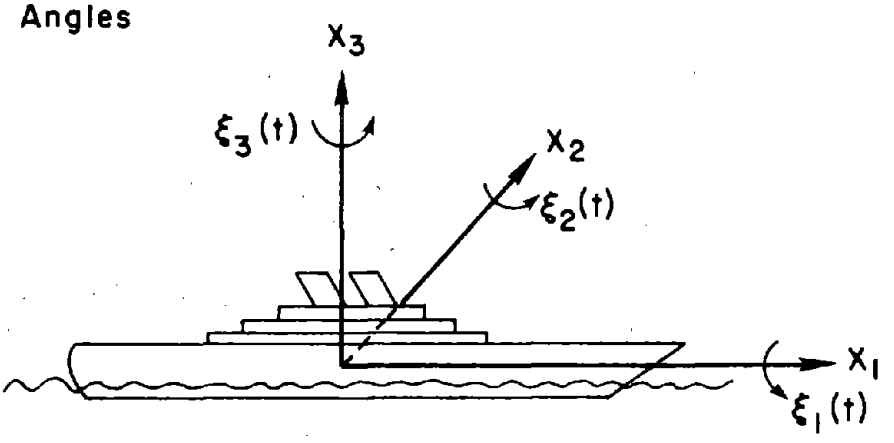

Figure 2 Typical Sample Function

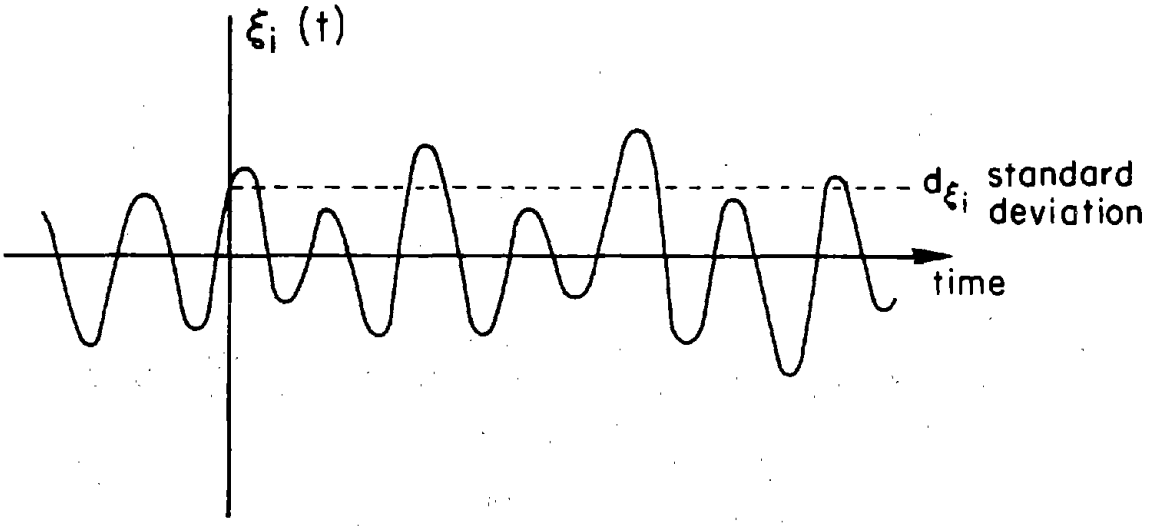

Table 1 Typical Standard Deviations (800 ft. vessel)

	Seastate			
	0	2	3	6
Roll $\sigma\xi_2$	0°	1-2°	5-6°	>10°
Pitch $\sigma\xi_2$	0°	2-3°	3-4°	4-6°
Yaw $\sigma\xi_3$	0°	0-1°	3-4°	5-8°

Table 2 Typical Periods of Rolling (mild seastate)

Vessel Type	Displacement (Tons)	Period (sec.)
Ocean Liners	30,000-50,000	20-28
Battleships	< 10,000	14-18
Heavy Cruisers	< 10,000	13-15
Destroyers	< 10,000	7-9
Patrol Boats	< 10,000	4-6

Figure 3 Ship and Antenna Geometry

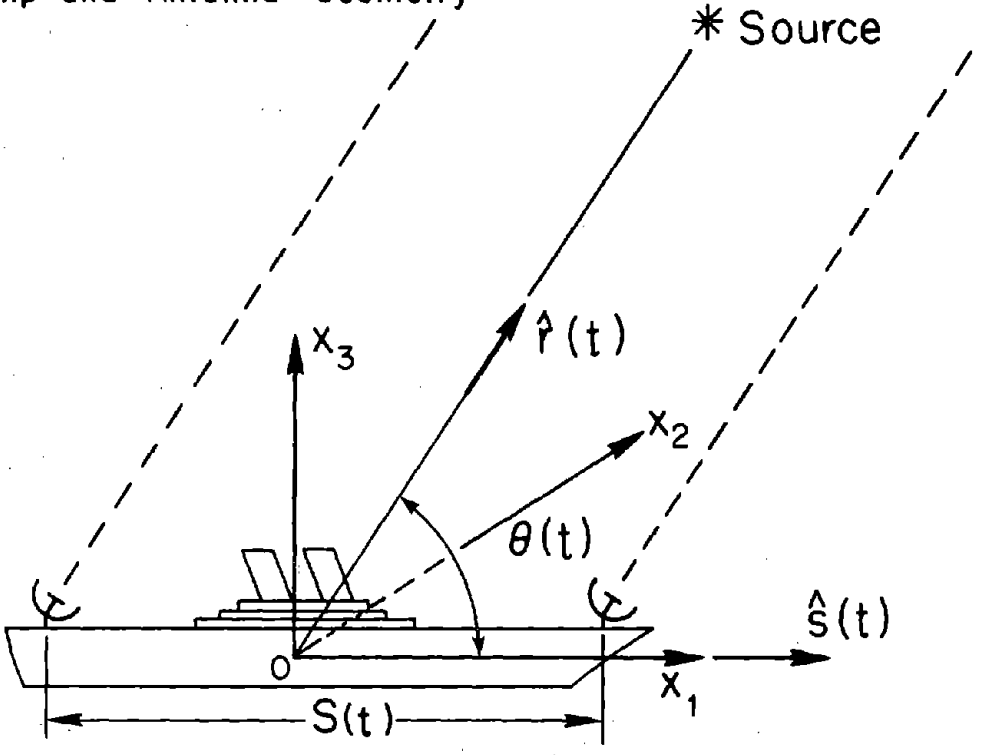

Figure 4 Accelerometer Placement

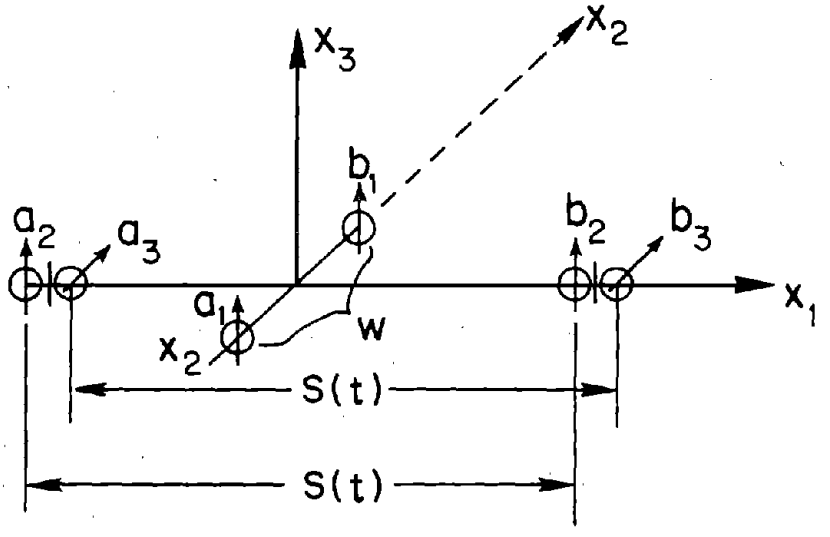

can be changed by as much as six fringe widths. It is, therefore, necessary to have a subsystem for monitoring accurately the length of the baseline. Several techniques are available for this purpose; one, for example, is to measure pulse return time on a taut, but stretchable, shorted transmission line. We will assume in the subsequent discussion that S(t) is known to within a fraction of a wavelength at all times.

The technique for determining the roll, pitch, and yaw angles of the interferometer baseline utilizes highly accurate accelerometers, placed judiciously on the vessel, as shown in Figure 4. The sensitivity-directions of these linear accelerometers are shown by the attached vectors. The magnitude of linear acceleration is given by $a_i(t)$ or $b_i(t)$, $i = 1,2,3$. The subscript (i) is related to the angular displacement ξ_i derived from the particular accelerometer's data. The first set of accelerometers is located along the x_2 axis, one on the starboard and one on the port side of the ship. The second and third sets of accelerometers, (a_2,b_2) and (a_3,b_3), are located at the antenna positions. The roll, pitch and yaw angles are obtained by "integrating" the differential equations

$$S(t)\ \frac{d^2\xi_i}{dt^2} + 2\frac{ds}{dt}\frac{d\xi_i}{dt} = \left[a_i(t) - b_i(t)\right] \qquad (1)$$

for $t = 2,3$ with appropriate initial conditions on $\xi_i(t)$. The equation for $\xi_1(t)$ contains the distance W(t) between the accelerometers a_1 and b_1 and there is no cross-product term $\frac{dW}{dt}\ \frac{d\xi_1}{dt}$.

The extent to which the time dependence of the length of the baseline, S(t), and the time dependence of W is significant depends on thermal

and mechanical stresses. Data on these factors will have to be obtained before we pass judgment on the question.

To a first order approximation in which we neglect the cross-term $\frac{ds}{dt}\frac{d\xi_1}{dt}$ the angles $\xi_i(t)$ are given by

$$\xi_1(t) = \int_0^t \int_0^\tau \frac{[a_1(\eta) - b_1(\eta)]}{W(\eta)} \, d\eta \, d\tau \tag{2}$$

$$\xi_2(t) = \int_0^t \int_0^\tau \frac{[a_2(\eta) - b_2(\eta)]}{S(\eta)} \, d\eta \, d\tau \tag{3}$$

$$\xi_3(t) = \int_0^t \int_0^\tau \frac{[a_3(\eta) - b_3(\eta)]}{S(\eta)} \, d\eta \, d\tau \tag{4}$$

on the assumption that

$$\xi_i(0) = \xi_i'(0) = 0 \qquad i = 1,2,3 \tag{5}$$

The desired accuracy of the measured roll angle, $\xi_1(t)$, is not extremely critical because rotation about the interferometer's baseline does not affect the fringe pattern. Rolling motion will, however, shift the position of the source in the main beams of the element-antennas of the interferometer. The angles ξ_1, ξ_2 and ξ_3 are needed

to slowly track the two antennas to compensate for the ship's motion and keep the position of the source fairly constant in their main beams. For this reason the error in the determination of $\xi_1(t)$ should be much smaller than the main beam-width. Typical beam-widths at centimeter wavelengths for moderate size parabolic reflectors are usually of the order of a few minutes of arc. For a 5 meter reflector and $\lambda = 1$ cm we have $\theta_{\frac{1}{2}} \approx 7$ min. The required accuracy of the pitch and yaw angles is much more stringent. These angles are used not only in the antenna tracking scheme but also in the data-processing scheme for determining the ship's position from the measurements of the phase-correlation of the waves from the source detected by the two antennas of the interferometer. The error-tolerance of the pitch and yaw angles must be less than a fringe width, which at centimeter wavelengths is of the order of magnitude of several seconds of arc. The use of highly accurate accelerometers located at the antennas should give $\xi_2(t)$ and $\xi_3(t)$ with very small error. Note that in this procedure that we have just sketched even the effects of bending of the baseline due to lack of perfect rigidity of the vessel are included in the measurements.

2.2 Coordinate Systems and Transformations

We need to use three fundamental coordinate systems in developing the theory of navigation by means of the interferometer. These systems which we name (a) the local horizon system, (b) the latitude-longitude system and (c) the celestial system are shown in Figures 5, 6, and 7, respectively. In the local system, Figure 5, the x', y', and z' cartesian axes are oriented in the due West, due South, and zenith direc-

tions, respectively. The orientation angles of the unit baseline vector, $\hat{s}'(t)$, are given by the azimuth and elevation angles, A(t) and E(t), respectively, as shown in Figure 5. These angles should be monitored at all times and are given by

$$A(t) = \xi_3(t) + \pi + p_o(t) \tag{6}$$

$$E(t) = -\xi_2(t) \tag{7}$$

where

$\xi_2(t)$ = pitch angle

$\xi_3(t)$ = yaw angle

$p_o(t)$ = ship bearing (East of North)

The "apparent" source position unit vector, $\hat{r}_a'(t)$, points in the direction that the source appears to be located with respect to the ship. This apparent source position may differ from the actual source position, represented by the unit vector $\hat{r}'(t)$, because of atmospheric effects. These effects will be considered in more detail in the following section where an approximate linear transformation between $\hat{r}'(t)$ and $\hat{r}_a'(t)$ will be derived by means of ray-theory on the basis that the effect is ascribable to refraction by the atmosphere. Note that the exact cartesian components of $\hat{r}'(t)$ or $\hat{r}_a'(t)$ are not known a priori in the local horizon system.

In the latitude-longitude coordinate system, Figure 6, the xy plane is the equatorial plane of the earth while the yz plane is the Greenwich meridian plane and the z axis is the polar axis. The orientation angles, δ and λ, of the unit vector, $\hat{z}'$, in the direction of the zenith relative to the ship, are the latitude and longitude angles, respectively, of the position of the ship on the earth. It is these angles which the interferometer navigational system will supply to a very high degree of accuracy. The unit vector, $\hat{s}'_o(t)$, is parallel to the x'y' plane and corresponds to the rest position that the unit baseline vector, $\hat{s}'(t)$, would have on a perfectly calm sea. The azimuth and elevation angles of this unit baseline "rest position" vector are given by

$$A_o(t) = \pi + p_o(t) \tag{8}$$

$$E_o(t) = 0 \tag{9}$$

The cartesian components of $\hat{s}'(t)$ and $\hat{s}'_o(t)$ will be known at all times during the operation of the interferometer-navigational-system and are given by

$$s'_x(t) = \sin A(t) \cos E(t) \tag{10}$$

$$s'_y(t) = \cos A(t) \cos E(t) \tag{11}$$

$$s'_z(t) = \sin E(t) \tag{12}$$

Figure 5 Local Horizon Coordinates

Figure 6 Latitude-Longitude Coordinates

and

$$s'_{x_o}(t) = \sin A_o(t) \tag{13}$$

$$s'_{y_o}(t) = \cos A_o(t) \tag{14}$$

$$s'_{z_o}(t) = 0 \tag{15}$$

The equivalent latitude and longitude angles of the actual source position are given by δ_s and λ_s, respectively. These angles can be found at any time using the tabulated declination and right ascension of the particular source being considered. The cartesian components of the unit position vector of the actual source, $\hat{r}(t)$, can be obtained using

$$r_x(t) = \sin \lambda_s(t) \cos \delta_s \tag{16}$$

$$r_y(t) = \cos \lambda_s(t) \cos \delta_s \tag{17}$$

$$r_z(t) = \sin \delta_s \tag{18}$$

Note that the exact cartesian components of the unit baseline vectors $\hat{s}(t)$ and $\hat{s}_o(t)$ are not known a priori. It will be shown that simultaneous knowledge of the cartesian components of any vector in both the local horizon system and the latitude-longitude system is equivalent to knowledge of the position of the ship on the earth.

The celestial coordinate system is shown in Figure 7. The x"-axis points in the direction of the vernal equinox which is also referred to as the "first point of Aries." (Years ago this axis was oriented towards the constellation Aries while at present, due to precession of the earth's polar axis, the x" axis points towards the constellation Pisces.) The x"y" plane is the equatorial plane and the z" axis is colinear with the z axis of the latitude-longitude system. The position angles of the actual source location, α_s and δ_s, are the right ascension and declination angles, respectively. The angles will be known for any particular source using tabulated data obtainable from ground-based measurements of positions and appropriate correction procedures for the given epoch. A detailed description of the various standard coordinate systems and the procedure for making the necessary corrections in the position of a source for a given epoch using the ephemeris are given in many texts on optical or radio astronomy such as that by Kraus, [3, chapter 2].

The declination angle, δ_s, and the equivalent latitude angle, δ_s, are, of course, the same. The relationship between the right ascension angle, $\alpha_s(t)$, and the equivalent longitude angle, $\lambda_s(t)$, is shown in Figure 8. The angle, $\mu(t)$, measured in radians, is given by

$$\mu(t) = \frac{\pi}{12} (S.T. + E.T.) \tag{19}$$

where

S.T. = sidereal time

E.T. = ephemeris time

S.T. can be obtained directly from "The American Ephemeris and Nautical Almanac" or similar ephemeris. E.T. can be obtained from Greenwich mean time, G.M.T., using

$$E.T. = G.M.T. + \Delta T \tag{20}$$

where the correction term, ΔT, is given for the particular epoch in any standard ephemeris. The relationship between α_s and $\lambda_s(t)$ is, as shown in Figure 8,

$$\alpha_s + \lambda_s(t) = \mu(t). \tag{21}$$

Later in this report we will use explicitly the linear transformation between the cartesian components of a vector in the latitude-longitude system and those of the same vector in the local horizon coordinate system. This transformation can be represented in matrix from by

$$\overline{U}' = \overline{\overline{A}} \cdot \overline{U} \tag{22}$$

where $\overline{U}'$ and $\overline{U}$ are column vectors whose elements are the components of the given vector in the respective coordinate systems. The elements of the transformation matrix can be obtained easily by considering the total transformation to be composed of two successive unitary rotation transformations. Using the 1-2-3 representation, $x \leftrightarrow 1$, $y \leftrightarrow 2$, $z \leftrightarrow 3$, the transformation in (23) can be written as

Figure 7 Celestial Coordinates

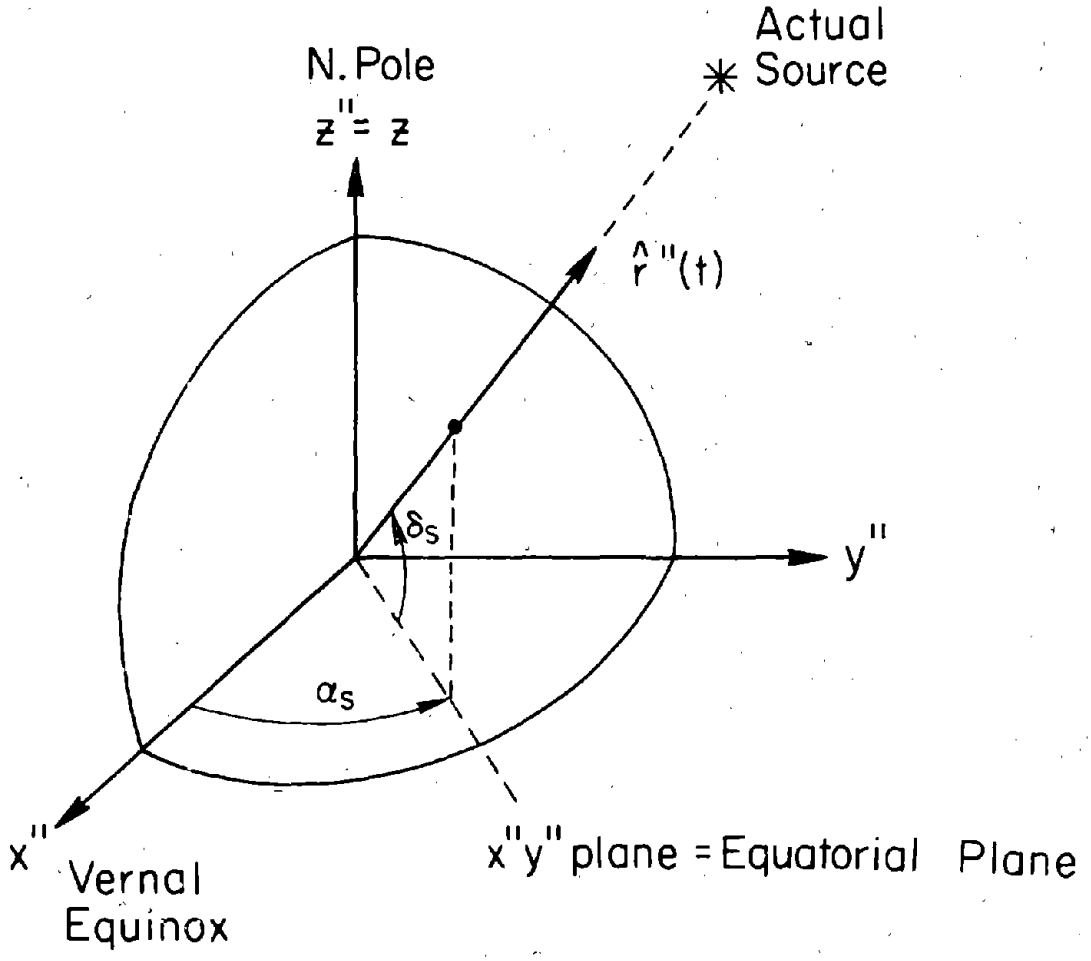

Figure 8 The Equatorial Plane

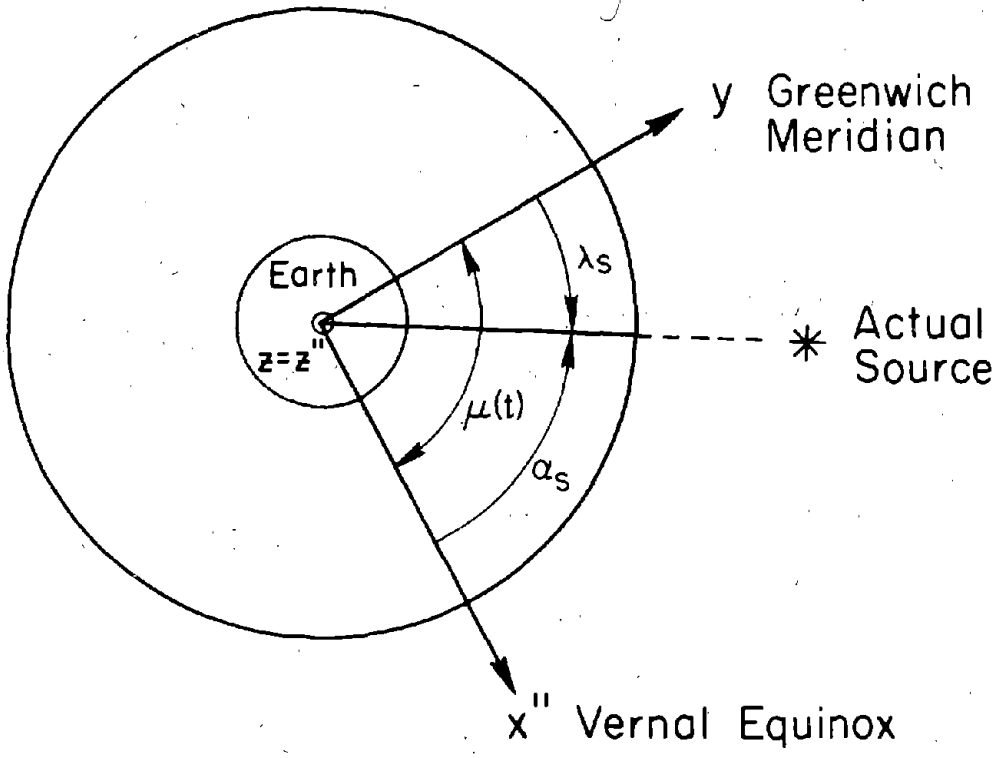

$$U_i' = \sum_{j=1}^{3} A_{ij} U_j \quad , \quad i = 1, 2, 3 \tag{23}$$

The elements of the transformation matrix, $\overline{\overline{A}}$, are given directly in terms of the latitude- and longitude-coordinates of the ship, $\delta(t)$ and $\lambda(t)$, respectively.

$$\overline{\overline{A}}(t) = \begin{bmatrix} \cos\lambda(t) & -\sin\lambda(t) & 0 \\ \sin\lambda(t)\sin\delta(t) & \cos\lambda(t)\sin\delta(t) & -\cos\delta(t) \\ \sin\lambda(t)\cos\delta(t) & \cos\lambda(t)\cos\delta(t) & \sin\delta(t) \end{bmatrix} \tag{24}$$

As was previously mentioned, the simultaneous knowledge of the cartesian components of any vector in both the horizon system and latitude-longitude system is equivalent to a knowledge of the ship's location on the earth. We will now obtain equations of evolution of the terms in this transformation matrix. These equations will be needed at a later time. We note that the latitude and longitude angles may be expressed in the form

$$\delta(t) = \delta(t_o) + \Delta\delta(t) \tag{25}$$

$$\lambda(t) = \lambda(t_o) + \Delta\lambda(t) \tag{26}$$

The changes of these angles may be obtained by considering the motion of the vessel on the planar projected latitude-longitude curvilinear coordinates shown in Figure 9. The equations of evolution of these

position coordinates of the ship are given by

$$\delta(t) = \delta(t_o) + \frac{1}{R} \int_{t_o}^{t} v(\tau) \cos p_o(\tau)\, d\tau \tag{27}$$

$$\lambda(t) = \lambda(t_o) - \frac{1}{R} \int_{t_o}^{t} v(\tau) \sec \delta(\tau) \sin p_o(\tau)\, d\tau \tag{28}$$

where $p_o(t)$ = measured bearing of ship (E of N), (radians)

$v(t)$ = measured speed of the ship, (m/sec)

R = radius of the earth, (meters)

We now substitute (27) and (28) into the matrix elements of (24) and use the angle sum formulas. Defining

$$f_1(t) \triangleq \cos\left(\frac{1}{R} \int_{t_o}^{t} v(\tau) \sec \delta(\tau) \sin p_o(\tau)\, d\tau\right) \tag{29}$$

$$f_2(t) \triangleq \sin\left(\frac{1}{R} \int_{t_o}^{t} v(\tau) \sec \delta(\tau) \sin p_o(\tau)\, d\tau\right) \tag{30}$$

and

$$g_1(t) \triangleq \cos\left(\frac{1}{R} \int_{t_o}^{t} v(\tau) \cos p_o(\tau)\, d\tau\right) \tag{31}$$

Figure 9 Planar Projected Latitude - Longitude Curvilinear Coordinates

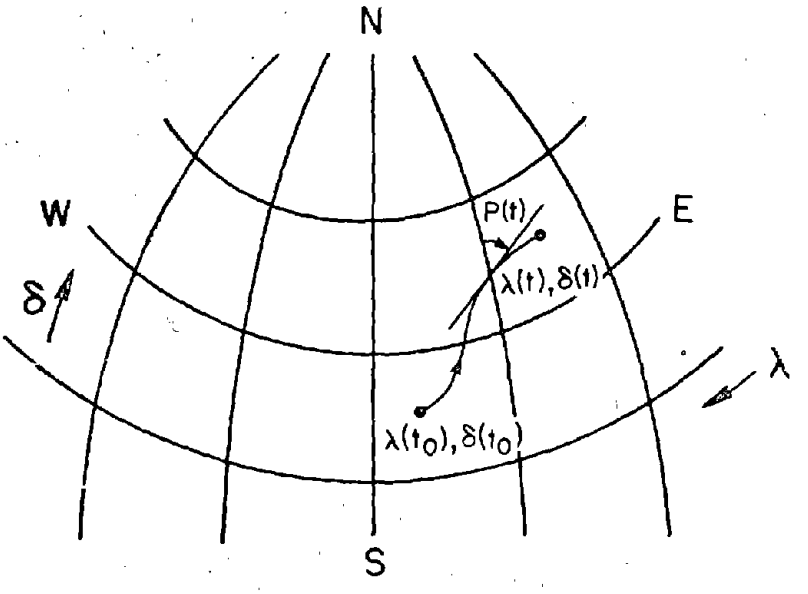

$$g_2(t) \triangleq \sin\left(\frac{1}{R}\int_{t_o}^{t} v(\tau)\cos p_o(\tau)\,d\tau\right) \tag{32}$$

and using the abbreviations

$$a_{ij}(t_o) = a_{ij_o} \qquad i, j = 1, 2, 3 \tag{33}$$

we obtain the equations of evolution

$$a_{11}(t) = f_1 a_{11_o} + f_2 a_{12_o} \tag{34}$$

$$a_{12}(t) = f_1 a_{12o} - f_2 a_{11o} \tag{35}$$

$$a_{21}(t) = f_1 g_1 a_{21_o} - f_1 g_2 a_{31_o} + f_2 g_1 a_{22_o} - f_2 g_2 a_{32_o} \tag{36}$$

$$a_{22}(t) = f_1 g_1 a_{22_o} - f_1 g_2 a_{32_o} - f_2 g_1 a_{21_o} + f_2 g_2 a_{31_o} \tag{37}$$

$$a_{23}(t) = g_1 a_{23_o} - g_2 a_{33_o} \tag{38}$$

$$a_{31}(t) = f_1 g_1 a_{31o} + f_1 g_2 a_{21_o} + f_2 g_1 a_{32_o} + f_2 g_2 a_{22_o} \tag{39}$$

$$a_{32}(t) = f_1 g_1 a_{32_o} + f_1 g_2 a_{22_o} - f_2 g_1 a_{31_o} - f_2 g_2 a_{21_o} \tag{40}$$

$$a_{33}(t) = g_1 a_{33_o} + g_2 a_{23_o} \tag{41}$$

2.3 The Refraction Matrix Approximation

As was mentioned in the previous section we will now derive an approximate linear matrix transformation between the unit vector, $\hat{r}'(t)$, in the direction of the actual source-position and the unit vector, $\hat{r}_a'(t)$, in the direction of the apparent source-position, using ray theory. The ray path in the earth's atmosphere of an incident monochromatic plane wave of frequency ω is shown in Figure 10. The curved ray path taken by the incident field will be determined by Fermat's principle [4, p. 356].

$$\delta \int_s n(\bar{r}, \omega)\, ds = 0 \tag{42}$$

where

$n(\bar{r}, \omega)$ = index of refraction as a function of position and frequency.

If $n(\bar{r}, \omega)$ is a known function the variational equation in (43) may be solved for the optical path, s, using the Euler-Lagrange equations. At the position of the ship on the surface of the ocean the incident field will appear to be coming from the direction, $\hat{r}_a'(t)$. The error angle between the actual and apparent source directions is given by ε. If we assume that the refractive index is only a function of height above the earth, with no horizontal gradients, then it can be shown, [5, pp. 82-87], that the error angle, ε, is given by the integral

$$\varepsilon = \int_1^{n_s} \cot \chi \frac{dn}{n} \approx \int_1^{n_s} \cot \chi \, dn \tag{43}$$

where n_s is the surface index of refraction and χ is the angle of the ray path with respect to the horizontal, as shown in Figure 10. If we assume that $n \approx 1$ along the path, (since $n_s \approx 1.0003$), the approximate form on the R.H.S. of Equation (44) is obtained. Substituting the refractivity

$$N \triangleq (n - 1) \times 10^6 \tag{44}$$

into (44) and integrating by parts we obtain

$$\varepsilon = 10^{-6} \int_0^{N_s} \cot \chi \, dN = 10^{-6} \left\{ N_s \cot \chi_s + \int_{\chi_0}^{\chi_s} \frac{N}{\sin^2 \chi} d\chi \right\} \tag{45}$$

2.4 Time-Domain Antenna Response

In this section we treat briefly the "voltage"-response* of an antenna to a source that is moving slowly through its main beam in terms of a quasi-static time-varying linear system approximation. The

---

*When the line into which the antenna feeds energy is a waveguide in which the dominant mode is one other than a TEM-mode the transmission line voltage and current require special definitions. This is well-known and treated in a number of books; for example, see R. E. Collin [6, pp. 145-197].

Figure 12 Moving Antenna Geometry

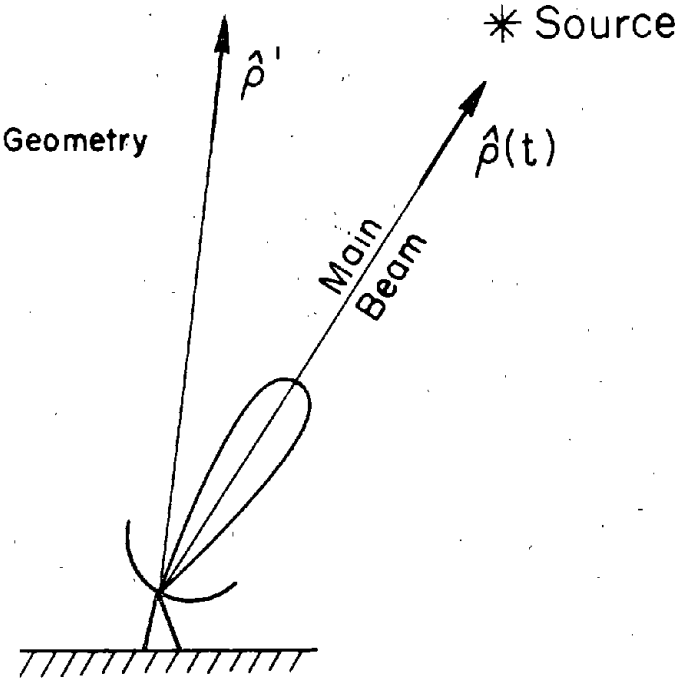

Figure 13 Equivalent Time-Varying Linear System

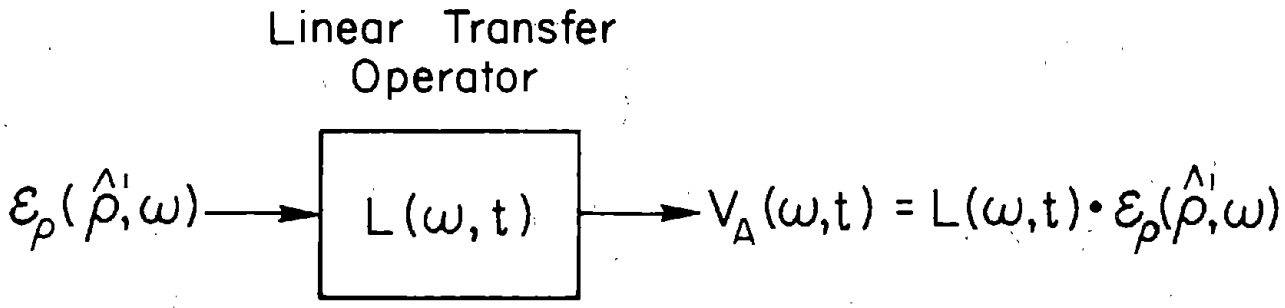

distant celestial source and the moving antenna are shown in Figure 12, where the position of the source is to be regarded as being fixed in the chosen coordinate system. The unit vector $\hat{\rho}(t)$ points in the direction of the center (axis) of the main beam of the antenna at a given angular frequency of operation $\underline{\omega}$. The unit vector $\hat{\rho}'$ is a "dummy" direction-vector. The equivalent time-varying linear system for the antenna and all sources of frequency $\underline{\omega}$ in all directions is shown diagrammatically in Figure 13. The driving term for the time-varying linear system operator, $L(\omega, t)$, is the Fourier time-transform of all incident electric fields of the particular polarization to which the antenna responds; we designate this quantity by $E_\rho(\hat{\rho}', \omega)$. The output of the system, $V_A(\omega, t)$, is not a true Fourier transform because it contains a slowly varying time-dependence. The time-domain response of the receiving system is obtained from $V_A(\omega, t)$ by inverse Fourier transformation.

$$V_A(t) = \frac{1}{2\pi} \int_{-\infty}^{\infty} V_A(\omega, t)\, e^{j\omega t}\, d\omega \tag{54}$$

The time-dependent linear operator, $L(\omega, t)$, involves an integration over all solid angles of the Fourier time-transforms of the incident electric fields of particular polarization that the antenna is sensitive to, weighted by an "antenna response function," $A(\hat{\rho}(t), \hat{\rho}', \omega)$.

$$V_A(\omega, t) = \iint_{\Omega} \varepsilon_\rho(\rho', \omega)\, A(\hat{\rho}(t), \hat{\rho}', \omega)\, d\Omega \tag{55}$$

This antenna response function has a magnitude that is proportional to the square root of the antenna power pattern, $\rho(\hat{\rho}(t), \hat{\rho}', \omega)$. In the case of celestial sources the incident spectrum $\varepsilon_\rho(\rho', \omega)$ will, of course, be unknown, or, at best, will be known statistically since the processes that generate these incident fields are random in nature.

If we feed the antenna voltage into a narrow band-pass R.F. amplifier, as shown in Figure 14, having a transfer function as shown in Figure 15, output voltage of the amplifier, in the time-domain, may be expressed in the form

$$v_{R.F.}(t) = \beta(t)\left[V_c(t)\cos\omega_o t - V_s(t)\sin\omega_o t\right] + N_s(t) + N_R(t) \quad (56)$$

The first term in the R.H.S. of (56) is the output due to the particular source being observed; it consists of the portion of the integral in (55) over only the extent of the source being passed through the narrow band R.F. amplifier with center frequency at ω_o. The terms in the brackets are one of the canonical representation for a narrowband signal, [7, pp. 132-136]. In this case this bracketed term represents the narrowband random signal due to the source when the antenna is not moving. The $\beta(t)$ multiplier represents the very slowly changing amplitude variation of the received signal that is due to the motion of the antenna pattern. The second term in (56), $N_s(t)$, is an undersired narrowband "noise" term generated by the extended integration in (55) over all sources other than that being observed. This term should be kept relatively small by using a highly directive antenna with very small side lobes and by observing a strong source in a sparsely occupied

Figure 14 Bandpass R.F. Amplifier

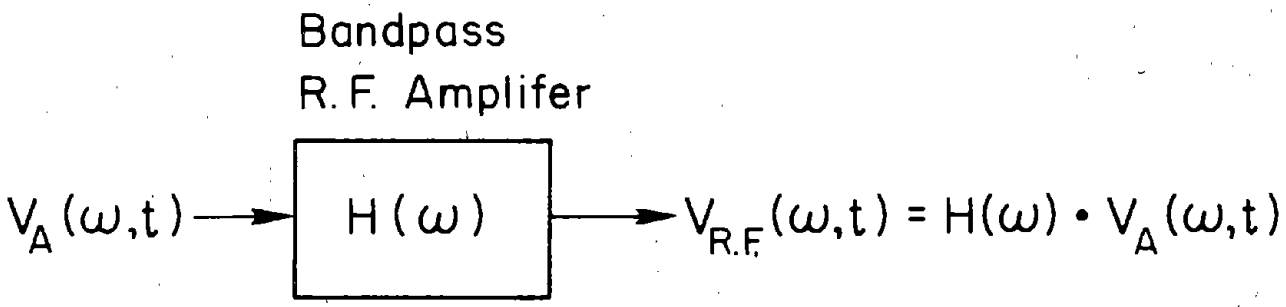

Figure 15 R.F. Amplifier Transfer Function

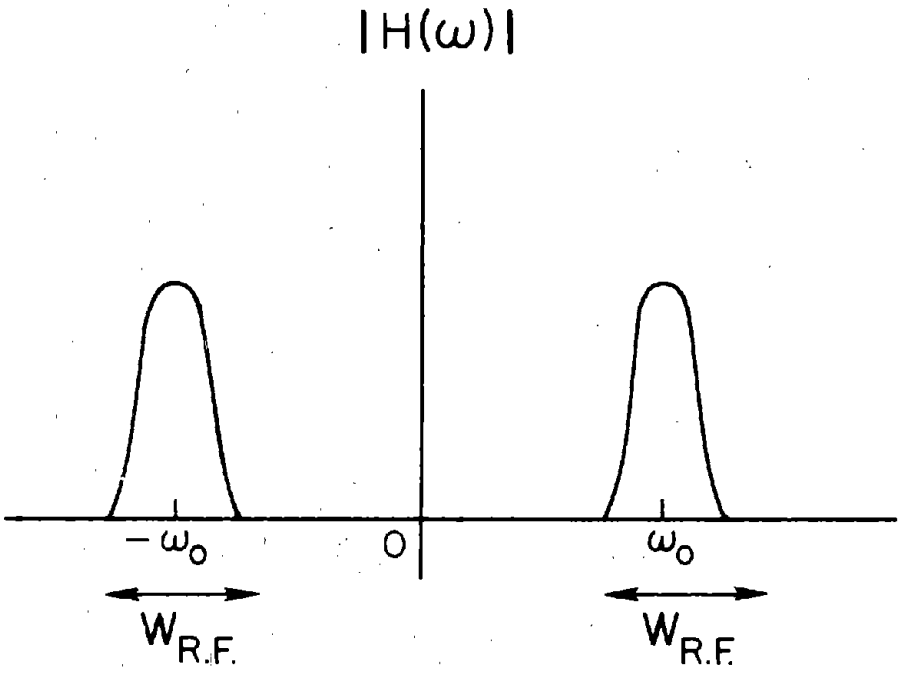

region of the celestial sphere. The tird term in (56), $N_R(t)$, is thermal noise generated in the receiver which appears in the output of the R.F. amplifier. This term will depend upon the structure and temperature of the various stages of the entire receiver including the antenna and R.F. amplifier. The interferometer system, to be discussed in the following chapter, incorporates two predetection antenna/receiver subsystems. The $N_R(t)$ generated by each of these two predetection subsystems are statistically independent and hence uncorrelated. The use of the correlation detection system will eliminate most of the uncorrelated thermal noise but will not eliminate the correlated, but undesired, noise terms, $N_s(t)$.

2.5 Antenna Tracking Equations

In the preceding section there appeared a multiplicative term, $\beta(t)$, that represented the variation in the amplitude of the received signal induced by the changing position of the source in the power pattern or "antenna response function," $A(\hat{\rho}(t), \hat{\rho}', \omega)$, of the antenna. For a ship on the ocean this relative motion of the source in the antenna's power pattern is induced by both the rotation of the earth and the motion of the ship on the sea. If the antenna does not track on the source to compensate for the roll, pitch, and yaw motions of the ship, considerable signal-amplitude variations can result. These amplitude variations will be roughly periodic in nature, at least for an axially symmetric main beam power pattern, and will have a periodicity of the order of the mean value of the roll, pitch and yaw periods. The magnitude of this amplitude variation will depend upon the ratio of the

roll, pitch and yaw angle variations to the main beam width of the antenna.

In this section we will develop tracking equations to keep the source in a relatively constant location in the main beam of the antenna. For antenna beamwidths smaller than the supremum of the standard deviations, δ_{ξ_1}, δ_{ξ_2}, δ_{ξ_3} in a given seastate, it will be mandatory for the antennas of the interferometer-navigational-system to track on the source and at least partially compensate for the ship's motion. The equations which we shall develop in this section will be based on assumed initial values of the coordinates of the position of the ship. This assumed position could be based on initial conventional navigational procedures during the startup of the interferometer or could be based on highly accurate position-fixes obtained previously by the interferometer system.

The right ascension and declination of a given discrete source will be known in the celestial coordinate system of Figure 7. The cartesian components of this source direction can be obtained in the latitude-longitude system of Figure 6 by calculating the equivalent longitude angle using (21) and also using the fact that δ_s = DEC. We then use equations (16), (17), and (18) to obtain the cartesian components of $\hat{r}(t)$. What we desire is an expression for the assumed (or actual) apparent position of the source in the local horizon system of Figure 5 using an initial guess (or knowledge) of the position of the ship on the earth. If this assumed (or known) position is given by the longitude and latitude angles, $\lambda_o(t)$ and $\delta_o(t)$, respectively, we may then obtain the assumed actual source position unit vector,

$\hat{r}'_o(t)$, in the local horizon system by substituting $\lambda_o(t)$ and $\delta_o(t)$ into the $\overline{\overline{A}}(t)$ matrix in equation (24). This gives us the approximate (or actual) transformation $\overline{\overline{A}}_o(t)$, and we obtain

$$\hat{r}'_o(t) = \overline{\overline{A}}_o(t) \circ \hat{r}(t) \tag{57}$$

To obtain the cartesian components of the assumed apparent position unit vector, $\hat{r}'_{a_o}(t)$, we use the assumed refraction matrix, $\overline{\overline{R}}_o(t)$, given in (53), where, from measurements, the surface refractivity is known and we use assumed (or actual) values ε_o and A_{s_o}. From (46) we have

$$\varepsilon_o(t) = 10^{-6} N_s \frac{\sqrt{r'^2_{x_o} + r'^2_{y_o}}}{r'_{z_o}} \tag{58}$$

and from equations (49) and (50)

$$A_{s_o}(t) = \tan^{-1}\left(\frac{r'_{x_o}}{r'_{y_o}}\right) \tag{59}$$

The assumed apparent position unit vector, $\hat{r}'_{a_o}(t)$, is then given by

$$\hat{r}'_{a_o}(t) = \overline{\overline{R}}_o(t) \circ \overline{\overline{A}}_o(t) \circ \hat{r}(t) \tag{60}$$

This vector gives the direction in which the optical axes of the interferometer antennas should be pointed. To track the antennas in this

Figure 16 The "Rest" and "Moving" Ship Coordinate Systems

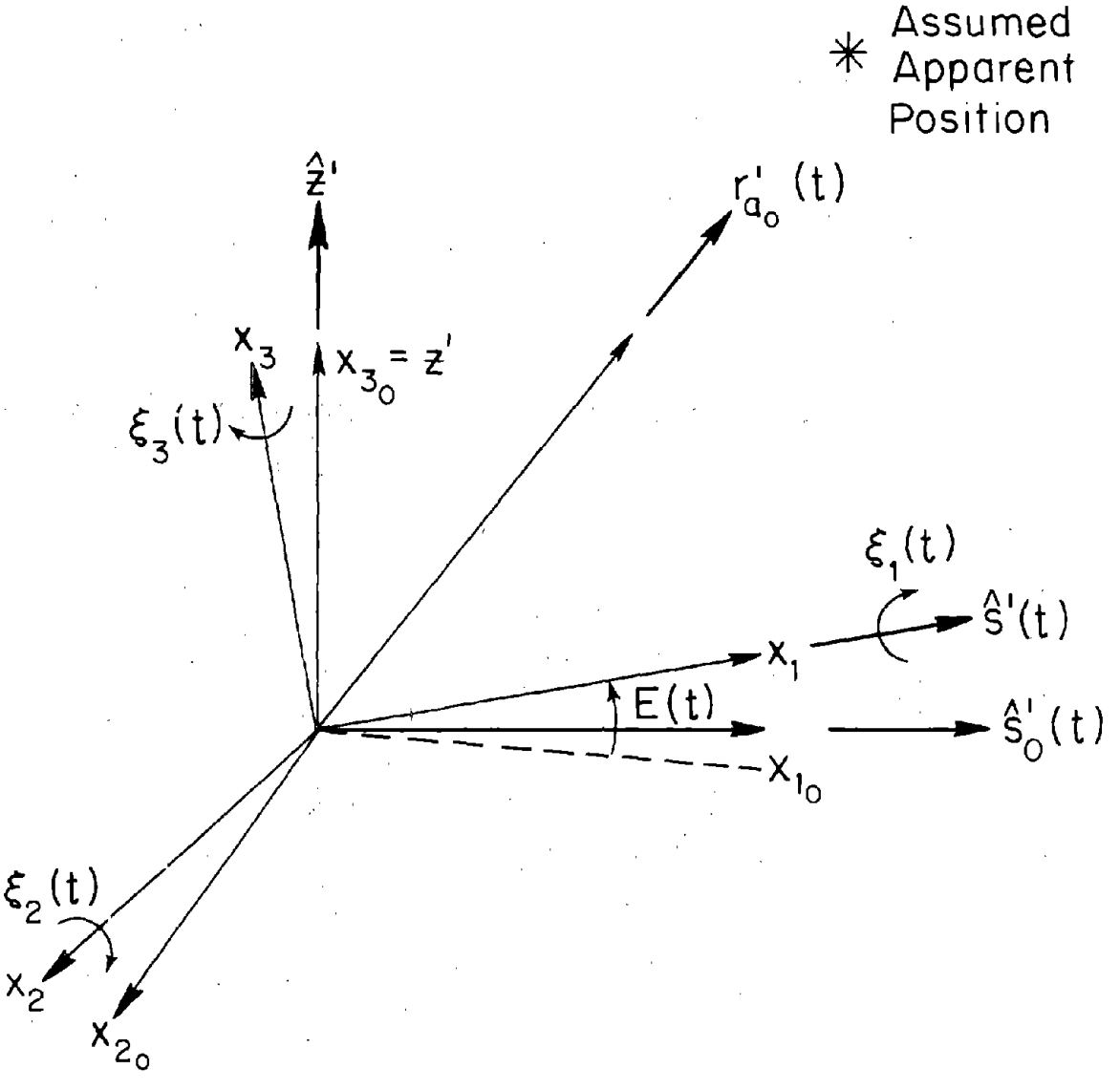

direction we will need equations of motion for direction coordinates that are fixed with respect to the ship. These coordinates are the longitudinal, transverse and zenith coordinates defined previously for both the "rest" and "moving" ship positions as shown in Figure 16. The coordinate system x_1, x_2, x_3 is the same as that shown in Figure 1 and moves with the ship. The system x_{1_o}, x_{2_o}, x_{3_o} defines the coordinates that the ship would have on a perfectly calm sea. The roll pitch and yaw angles, $\xi_1(t)$, $\xi_2(t)$, and $\xi_3(t)$, are assumed to be known at all times using the techniques described in section 2.1.

What we will now obtain are the cartesian components of the assumed apparent position unit vector of the source in the "moving" coordinate system (x_1, x_2, x_3). By means of this information it will be possible to transform to any convenient angular coordinate system attached to the ship (and the antenna mounts), such as a local altitude-azimuth system, to continually track on the assumed (or actual) source-position. By using this scheme we shall get direct equations of motion that not only consider the rotation of the earth but also all motions of the ship on the sea. We obtain the final transformation in two more steps. The first of these is a coordinate transformation from the local horizon system to the rest-position-cartesian system. It is apparent by inspection of Figure 5 that this transformation is given by the matrix

$$\overline{\overline{T}}_1(t) = \begin{bmatrix} \cos A_o(t) & -\sin A_o(t) & 0 \\ \sin A_o(t) & \cos A_o(t) & 0 \\ 0 & 0 & 1 \end{bmatrix} \qquad (61)$$

We now will obtain the transformation matrix from the "rest" system to the moving system. This can be done in three successive rotations, one for each angle $\xi_1(t)$, $\xi_2(t)$ and $\xi_3(t)$. The total transformation matrix is the product of these successive rotational transformations. Using Figure 16 the individual rotation transformations can be obtained by inspection. The total transformation is thus found to be

$$\overline{\overline{T}}_2(t) = \begin{bmatrix} 1 & 0 & 0 \\ 0 & \cos\xi_1 & \sin\xi_1 \\ 0 & -\sin\xi_1 & \cos\xi_1 \end{bmatrix} \begin{bmatrix} \cos\xi_2 & 0 & -\sin\xi_2 \\ 0 & 1 & 0 \\ \sin\xi_2 & 0 & \cos\xi_2 \end{bmatrix} \begin{bmatrix} \cos\xi_3 & \sin\xi_3 & 0 \\ -\sin\xi_3 & \cos\xi_3 & 0 \\ 0 & 0 & 1 \end{bmatrix} \quad (62)$$

If we denote the assumed apparent position-unit-vector as $\hat{r}_{a_o}(t)$ in the x_1, x_2, x_3 coordinate system attached to the ship, this vector can be found at any time t from

$$\hat{r}_{a_o}(t) = \overline{\overline{T}}_2 \circ \overline{\overline{T}}_1 \circ \overline{\overline{R}}_o \circ \overline{\overline{A}}_o \circ \hat{r}(t) \quad (63)$$

All calculations involved in this equation can be done by a computer and the antennas can be servo-controlled to track on this position. The motions of the antennas involved in this tracking procedure will be of a very small angular velocity such as one-tenth or two-tenths of a degree per second. Such tracking motions should not be difficult to realize. We will assume that such a tracking procedure is carried out for each of the two interferometer antennas. Such a tracking procedure will, to a very close approximation, make the term $\beta(t)$ for each

antenna a constant. This occurs because the position of the source in the antenna power pattern remains fairly constant even though it may not be located exactly in the middle of the power pattern owing to an initial slight error in the assumed ship position.

It will be assumed later that the term $\beta(t)$ at each antenna of the interferometer is never so small as to effectively extinguish the source signal when compared to the background noise at the output of the correlation receiver during the course of any measurement of position. The time involved in a single measurement is one or two minutes. The tracking procedure must therefore "initialize" the pointing of the antennas so that the source is well within the main beams of the antennas and then keep it there throughout the measurement of one or two minutes. The initial pointing, using (63), requires an a priori knowledge of the ship's position on the earth to within 1/3 or 1/4 of the main beamwidth of the antennas in both latitude and longitude coordinates. As an example, a dish 3 meters in diameter operating at f_o = 30 GHz will have a main beam width, $\theta_{\frac{1}{2}} \approx 3.3 \times 10^{-3}$ radians. When observations of the source are made, close to the zenith, on the basis of an assumed ship position to within about $\theta_{\frac{1}{2}}/3$ radians we are guaranteed that the source is initially located well within the main beam of the antenna. Thus λ_o and δ_o must be within about 1.1×10^{-3} radians $\doteq$ .0625 degrees of the true ship-position. This is equivalent to an initial knowledge of position to within about 4.3 miles of the true position. Of course, once the interferometer system is operating continuously the ship position will be known at all times to within a distance of one-hundredth, or a smaller fraction of the above figure.

III. THE INTERFEROMETER NAVIGATIONAL SYSTEM

3.1 Time-Varying Phase Path Differences

In this section we consider a very general formulation for representing the output voltages of the two antenna/R.F. amplifier "front ends" of the interferometer in terms of phase path differences. Consider the two antennas and R.F. amplifiers shown in Figure 17. The unit vectors, $\hat{r}'_a(t)$ and $\hat{s}'(t)$, are in the direction of the apparent source and along the baseline, respectively. The baseline distance is given by $S(t)$, and the angle $\Theta'(t)$ is the angle between $\hat{s}'(t)$ and $\hat{r}'_a(t)$. In vector notation we have

$$\hat{s}'(t) \cdot \hat{r}'_a(t) = \cos \Theta'(t) \tag{64}$$

As was shown in section 2.4, equation (56), the output voltages of the first and second bandpass R.F. amplifiers may be written in the forms

$$v_{RF_1}(t) = \beta_1(t) \left[V_{c_1}(t) \cos \omega_o t - V_{s_1}(t) \sin \omega_o t\right] + N_{s_1}(t) + N_{R_1}(t) \tag{65}$$

$$v_{RF_2}(t) = \beta_2(t) \left[V_{c_2}(t) \cos \omega_o t - V_{s_2}(t) \sin \omega_o t\right] + N_{s_2}(t) + N_{R_2}(t) \tag{66}$$

The terms $\beta_1(t)$ and $\beta_2(t)$ are slowly varying amplitude functions generated by the source moving through the main lobes of the antennas. If the antennas are identical and are always pointing in the same direction, we have $\beta_1(t) = \beta_2(t)$. If the antennas are tracking on the source so that the source position does not change in the main beams of the antennas,

Figure 17 Interferometer Phase Path Geometry

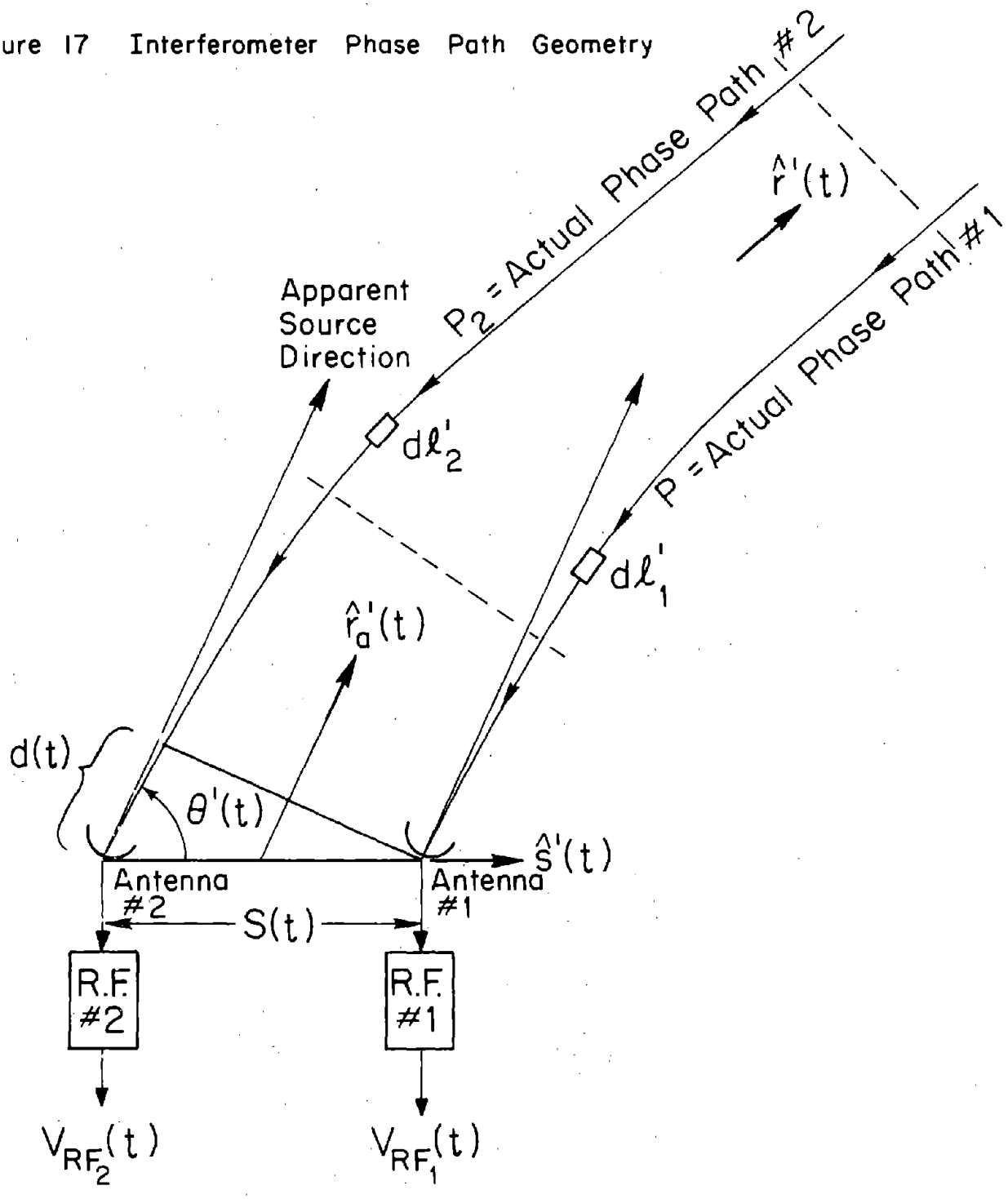

$\beta_1(t) = \beta_2(t) = \beta_o$, a constant term. The terms in the brackets represent narrow-band random signals generated by the incident fields from the source. These incident fields at each antenna differ by a time delay factor due to the different phase path lengths for the Fourier time components arriving at each antenna. If we assume that the R.F. amplifiers have identical *narrow-band* transfer functions, as shown in Figure 15, and that the frequency dependence of the index of refraction profile, $n(\bar{\ell}', \omega)$, is smooth in the frequency neighborhood of ω_o, then, to a close approximation, each Fourier component of the incident random, narrow-band source-signal will have the same time delay. We may then write

$$V_{c_2}(t) \cos \omega_o t - V_{s_2}(t) \sin \omega_o t = V_{c_1}(t - \tau) \cos \omega_o(t - \tau) - V_{s_1}(t - \tau) \sin \omega_o(t - \tau) \tag{67}$$

The time "delay," $\tau(t)$, is a function of time given by the difference between the phase path integrals from the source to the second and first antennas, respectively, divided by the free space velocity of light, c. Note that a negative "delay" corresponds to a time advancement of the signal at antenna #2 compared to the signal at antenna #1.

$$\tau(t) = \frac{1}{c} \left\{ \int_{P_2(t)} n(\bar{\ell}_2'(t), \omega_o)\, d\ell_2' - \int_{P_1(t)} n(\bar{\ell}_1'(t), \omega_o)\, d\ell_1' \right\} \tag{68}$$

Where P_2 and P_1 are the actual phase paths from the source to the second and first antenna, as shown in Figure 17, and $n(\bar{\ell}_2'(t), \omega_o)$ and $n(\bar{\ell}_1'(t), \omega_o)$

are the respective indices of refraction at the center frequency, ω_o, along the phase paths. We now replace the indices of refraction in equation (68) by their representations in terms of refractivity, N, using

$$n = 1 + N \times 10^{-6} \tag{69}$$

and note that to a very good approximation

$$\int_{P_2(t)} d\ell_2' = \int_{P_1(t)} d\ell_1' + d(t) \tag{70}$$

where d(t) is the straight line approximation to the last section of phase path, P_2, as shown in Figure 17. The result is

$$\tau(t) = \frac{d(t)}{c} + \frac{10^{-6}}{c} \left\{ \int_{P_2} N(\ell_2', \omega_o)\, d\ell_2' - \int_{P_1} N(\ell_1', \omega_o)\, d\ell_1' \right\} \tag{71}$$

Looking at Figure 17 we see that

$$d(t) = S(t) \cos \Theta'(t) = S(t)\ \hat{s}'(t) \cdot \hat{r}_a'(t) \tag{72}$$

which yields the formula

$$\tau(t) = \frac{S(t)}{c}\ \hat{s}'(t) \cdot \hat{r}_a'(t) + \Delta\tau(t) \tag{73}$$

where $\Delta\tau(t)$ is the second term on the R.H.S. of (71). If we assume that of the refractivity of the atmosphere is only a function of height (radially stratified model), the integrals in $\Delta\tau(t)$ over P_1 and $P_2 - d(t)$ are equal. If, then, we approximate $N(\ell_2', \omega_o)$ in the last section of integration in P_2, of length $d(t)$, by $N_s(t, \omega_o)$, the refractivity at the surface which is also, in general, a function of time, we obtain

$$\Delta\tau(t) \doteq \frac{10^{-6}}{c} N_s(t, \omega_o)\, d(t) \tag{74}$$

Substitution into (73) and the use of (69) and (72) yields

$$\tau(t) \doteq \frac{n_s(t, \omega_o)S(t)}{c} s'(t) \cdot \hat{r}_a'(t) \tag{75}$$

Let us define the time-varying phase difference

$$\phi(t) = \omega_o\tau(t) = \frac{n_s(t, \omega_o)S(t)\omega_o}{c} s'(t) \cdot \hat{r}_a'(t) \tag{76}$$

We may then rewrite (67) as

$$V_{c_2}(t) \cos \omega_o t - V_{s_2}(t) \sin \omega_o t =$$

$$V_{c_1}(t - \tau) \cos \left(\omega_o t - \phi(t)\right) - V_{s_1}(t - \tau) \sin \left(\omega_o t - \phi(t)\right) \tag{77}$$

The noise terms $N_{s_1}(t)$ and $N_{s_2}(t)$ are generated, as explained in section 2.4, by sources other than that observed. These two noise terms will be weakly correlated but will not differ by a simple time delay since they are each generated by fields incident from sources at all angles weighted by the antenna response function, as shown in equation (55).

The receiver noise terms, $N_{R_1}(t)$ and $N_{R_2}(t)$, are, in general, uncorrelated and their effects are greatly reduced by the correlation receiver to be described in the following section.

3.2 The Correlation Receiver

We proceed now to consider the operation of a basic correlation receiver to be used for navigation by observing a discrete radio source whose celestial coordinates are known as a function of time. In the following section we will present the technique for utilizing the interferometer and correlation receiver for navigation. The basic correlation receiver is shown in block diagram form in Figure 18. The output signals from the bandpass R.F. amplifiers are of the form given in the preceding section by equations (65) and (66).

$$v_{RF_1}(t) = \beta_1(t)\left[V_{c_1}(t)\cos\omega_o t - V_{s_1}(t)\sin\omega_o t\right] + N_{s_1}(t) + N_{R_1}(t) \quad (65)$$

$$v_{RF_2}(t) = \beta_2(t)\left[V_{c_2}(t)\cos\omega_o t - V_{s_2}(t)\sin\omega_o t\right] + N_{s_2}(t) + N_{R_2}(t) \quad (66)$$

For the interferometer navigational system to be described, we assume that the identical antennas making up the elements of the interferometer are tracking on the assumed source position so closely that the source stays well within the main beams. Therefore, the terms $\beta_1(t) = \beta_2(t) = \beta_o(t)$ change very, very slowly and never become so small that the signal from the source gets lost in the noise at the output of the correlation receiver. We assume also that the R.F. and I.F. amplifiers of both predetection subsystems have respectively identical bandpass

Figure 18 The Interferometer and Correlation Receiver

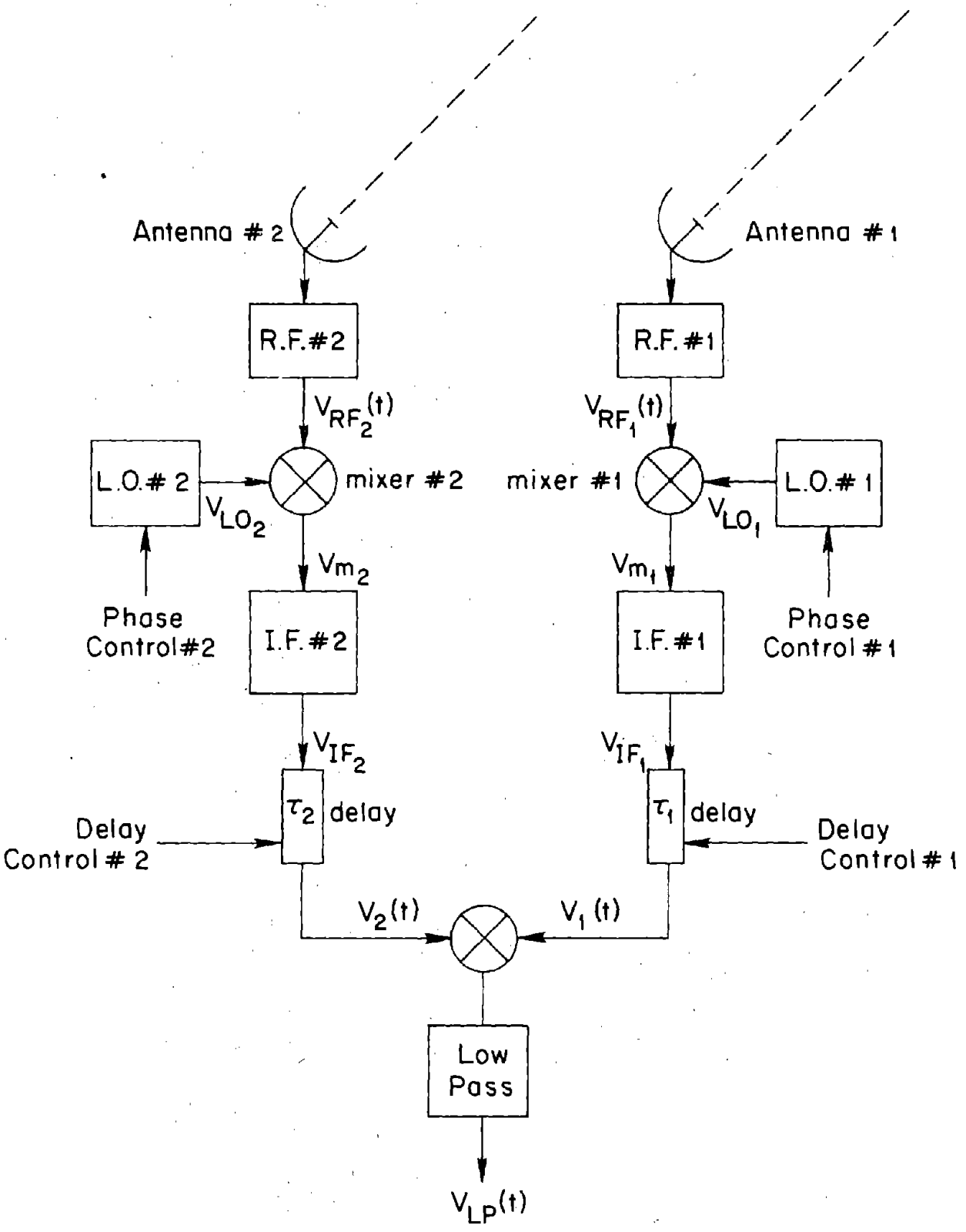

characteristics such as are shown in Figure 19 (p. 68). The R.F. amplifiers are "narrow-band"; the refractivity function, $N(\bar{\ell}', \omega)$, ω assumed to be smooth with respect to frequency in the neighborhood of ω_o. We can thus represent the relative variations of the two source-signals v_{RF_1} and v_{RF_2} by a simple time delay (or advancement) as explained in the previous section. Using equations (65), (66) and (77), we have

$$v_{RF_1}(t) = \beta_o(t) \left[V_{c_1}(t) \cos \omega_o t - V_{s_1}(t) \sin \omega_o t\right] + N_{s_1}(t) + N_{R_1}(t) \quad (78)$$

$$v_{RF_2}(t) = \beta_o(t) \left[V_{c_1}(t - \tau) \cos \left(\omega_o t - \phi(t)\right) - V_{s_1}(t - \tau) \sin \left(\omega_o t - \phi(t)\right)\right] + N_{s_2}(t) + N_{R_2}(t) \quad (79)$$

where from (75) and (76)

$$\tau(t) \doteq \frac{n_s(t, \omega_o)\, S(t)}{c}\, \hat{s}'(t) \cdot \hat{r}_a'(t) \quad (75)$$

$$\phi(t) \doteq \frac{\omega_o n_s(t, \omega_o)\, S(t)}{c}\, \hat{s}'(t) \cdot \hat{r}_a'(t) \quad (76)$$

The signals (78) and (79) are mixed with signals from the local oscillators as shown in Figure 18. These local oscillators are phase controlled with voltages given by

$$v_{Lo_1}(t) = 2 \cos \left[(\omega_o - \omega_{IF})\ t\right] \tag{80}$$

$$v_{Lo_2}(t) = 2 \cos \left[(\omega_o - \omega_{IF})\ t - \phi_o(t)\right] \tag{81}$$

The phase term $\phi_o(t)$ will be explained in the following section. The mixed signals are given by

$$v_{m_1}(t) = \beta_o(t) \left[V_{c_1}(t) \cos \omega_{IF}t - V_{s_1}(t) \sin \omega_{IF}t\right] + \left[N_{s_1}(t) + N_{R_1}(t)\right] v_{Lo_1}(t)$$

$$+ f_1\left((2\omega_o - \omega_{IF})\ t\right) \tag{82}$$

$$v_{m_2}(t) = \beta_o(t) \left[V_{c_1}(t - \tau) \cos \left(\omega_{IF}t + \Delta\phi(t)\right)\right.$$

$$\left. -V_{s_1}(t - \tau) \sin \left(\omega_{IF}t + \Delta\phi(t)\right)\right] + \left[N_{s_2}(t) + N_{R_2}(t)\right] v_{Lo_2}(t)$$

$$+ f_2\left((2\omega_o - \omega_{IF})\ t\right) \tag{83}$$

where

$$\Delta\phi(t) = \phi_o(t) - \phi(t) \tag{84}$$

and f_1 and f_2 are the upper side band terms at $2\omega_o - \omega_{IF}$ that will be eliminated when the signals pass through the I.F. filters. The signals at the I.F. outputs will have the forms

$$v_{IF_1}(t) = G_o\beta_o\left[V_{c_1}(t)\cos\omega_{IF}t - V_{s_1}(t)\sin\omega_{IF}t\right] + N_{IF_1}(t) \tag{85}$$

$$v_{IF_2}(t) = G_o\beta_o\left[V_{c_1}(t-\tau)\cos\left(\omega_{IF}t + \Delta\phi(t)\right) - V_{s_1}(t-\tau)\sin\left(\omega_{IF}t + \Delta\phi(t)\right)\right] + N_{IF_2}(t) \tag{86}$$

where G_o is the I.F. amplifier gain and $N_{IF_1}(t)$ and $N_{IF_2}(t)$ are the total non-signal noise terms at the outputs of respective I.F. amplifiers.

The time delays at the outputs of the I.F. amplifiers are controlled together to recorrelate the terms $V_{c_1}(t-\tau)$ and $V_{s_1}(t-\tau)$ in (86) with their non-delayed counterparts in (85). This can be done in one of two ways depending upon the sign of the "delay," $\tau(t)$. The sign of this term will be known even though its exact magnitude will be unknown when the ship's exact position is unknown. For $\tau > 0$ we set $\tau_2 = 0$ and set $\tau_1(t)$ to an assumed value for $\tau(t)$ based on the assumed ship-position. This is done using the assumed unit source direction vector, $\hat{r}_{a_o}(t)$, given in equation (63) of section 2.5. Denoting the assumed apparent position of the source in the local horizon frame by the unit vector, $\hat{r}'_{a_o}(t)$, we define, using (75),

$$\tau_o(t) \triangleq \frac{n_s(t,\omega_o)\,S(t)}{c}\,\hat{s}'(t)\cdot\hat{r}'_{a_o}(t) \tag{87}$$

Now, using the invariance of the scalar product and the fact that in the "moving" system attached to the ship the unit baseline vector has the representation $\hat{X}_1$, we obtain from (87)

$$\tau_o(t) = \frac{n_s(t, \omega_o)\, S(t)}{c} \left[\hat{r}_{a_o}(t)\right]_{X_1} \tag{88}$$

where the X_1 component of $\hat{r}_{a_o}(t)$ will be known using (64). Since $V_{c_1}(t)$ and $V_{s_1}(t)$ are random signals of bandwidth $\Delta\nu_{IF}$, their auto correlation coefficients approach zero very rapidly for time separations greater than $\frac{1}{\Delta\nu_{IF}}$. It is, therefore, mandatory that the error in $\tau_o(t)$ be only a fraction of $\frac{1}{\Delta\nu_{IF}}$. Substituting $n_s \approx 1$ and denoting the angles from the $\hat{s}'$ vector to the actual and assumed apparent unit direction vectors $\hat{r}'_a$ and $\hat{r}'_{a_o}$ as Θ'_a and Θ'_{a_o}, respectively, we obtain with $\left[\hat{r}_{a_o}\right]_X = \cos\Theta'_{a_o}$

$$\Delta\tau = \tau(t) - \tau_o(t) << \frac{1}{\Delta\nu_{IF}} \qquad \cos\Theta'_a - \cos\Theta'_{a_o} << \frac{\Delta\lambda_{IF}}{S(t)} \tag{89}$$

where $\Delta\lambda_{IF}$ is the equivalent wavelength of the I.F. bandwidth frequency. For observations near the zenith we expand the cosine functions in Taylor's series about $\Theta = \pi/2$. The result is

$$\Delta\Theta = \Theta'_{a_o} - \Theta_a << \frac{\Delta\lambda_{IF}}{S(t)} \qquad \text{(zenith observations)} \tag{90}$$

If we assume $\Delta\nu_{IF} = 200$ MHz and $S(t) = 200$ meters, we find, for example,

$$\Delta\Theta << 7.5 \times 10^{-3} \text{ radians} \doteq 26 \text{ min} \tag{91}$$

Requirements for accuracy of this order of magnitude will not introduce

additional problems in the procedure since use of the antenna tracking technique in section 2.5 requires a $\Delta\Theta_{max}$, that is, a fraction of the main beam width. Such antenna tracking requirements will usually satisfy the additional requirement in (89) easily.

For the case of $\tau < 0$ we set $\tau_1 = 0$ and set $\tau_2 = \tau_o(t)$. The time delay circuits in Figure 18 may consist of binary sequenced delay lines such as are now used in the Hat Creek interferometer system. In using such a discrete delay circuit the resolution must be kept small enough so that the error, $\Delta\tau$, is always less than $1/\Delta\nu_{IF}$.

The inputs into the final multiplier, $v_1(t)$ and $v_2(t)$, as shown in Figure 18, will have alternate forms, depending upon whether $\tau(t)$ is positive or negative. These forms are given, for $\tau > 0$ and $\tau < 0$, respectively, by $\tau > 0 \Rightarrow \tau_2 = 0$, $\tau_1 = \tau_o = \tau - \Delta\tau$

$$v_1(t) = G_o\beta(t - \tau_o)\Big[V_{c_1}(t - \tau + \Delta\tau)\cos\omega_{IF}(t - \tau_o) - V_{s_1}(t - \tau + \Delta\tau)\sin\omega_{IF}(t - \tau_o)\Big] + N_{IF_1}(t - \tau_o) \tag{92}$$

$$v_2(t) = G_o\beta(t)\Big[V_{c_1}(t - \tau)\cos(\omega_{IF}t - \Delta\phi) - V_{s_1}(t - \tau)\sin(\omega_{IF}t - \Delta\phi)\Big] + N_{IF_2}(t) \tag{93}$$

$\tau < 0 \Rightarrow \tau_1 = 0$, $\tau_2 = \tau_o = \tau - \Delta\tau$

$$v_1(t) = G_o\beta(t)\Big[V_{c_1}(t)\cos\omega_{IF}t - V_{s_1}(t)\sin\omega_{IF}t\Big] + N_{IF_1}(t) \tag{94}$$

$$v_2(t) = G_o\beta(t - \tau_o)\Big[V_{c_1}(t + \Delta\tau)\cos\left(\omega_{IF}(t - \tau_o) - \Delta\phi\right) - V_{s_1}(t + \Delta\tau)\sin\left(\omega_{IF}(t - \tau_o) - \Delta\phi\right)\Big] + N_{IF_2}(t - \tau_o) \qquad (95)$$

The paired inputs in (92) and (93) or (94) and (95) are now multiplied and the resultant put through the final low-pass filter or "integrator." The transfer function of this low-pass filter is shown in Figure 19. The products put into this filter are of the forms

$\tau > 0$

$$v_1(t)v_2(t) = G_o^2\beta(t)\beta(t - \tau_o) \times \left\{\left[\frac{V_{c_1}(t - \tau + \Delta\tau)\ V_{c_1}(t - \tau) + V_{s_1}(t - \tau + \Delta\tau)\ V_{s_1}(t - \tau)}{2}\right]\cos\ (\Delta\phi - \omega_{IF}\tau_o) + \left[\frac{V_{c_1}(t - \tau + \Delta\tau)\ V_{s_1}(t - \tau) - V_{c_1}(t - \tau)\ V_{s_1}(t - \tau + \Delta\tau)}{2}\right]\sin\ (\Delta\phi - \omega_{IF}\tau_o)\right\} + g(2\omega_{IF}t) + N_{o_1}(t) \qquad (96)$$

$\tau < 0$

$$v_1(t)v_2(t) = G_o^2\beta(t)\beta(t - \tau_o) \times \left\{\left[\frac{V_{c_1}(t + \Delta\tau)V_{c_1}(t) + V_{s_1}(t + \Delta\tau)V_{s_1}(t)}{2}\right]\cos\left(\Delta\phi + \omega_{IF}\tau_o\right) + \left[\frac{V_{c_1}(t + \Delta\tau)V_{s_1}(t) - V_{c_1}(t)V_{s_1}(t + \Delta\tau)}{2}\right]\sin\left(\Delta\phi + \omega_{IF}\tau_o\right)\right\} + h(2\omega_{IF}t) + N_{o_2}(t) \qquad (97)$$

The terms g and h represent upper side band terms at a frequency of $2\omega_{IF}$ that will be eliminated by the low-pass filter. The terms N_{o_1} and N_{o_2} are noise terms with bandwidths of $2\omega_{IF}$. When the product in (96) or (97) is passed through the low pass filter only the low frequency components of the noise terms will remain. The time average noise power is directly proportional to the noise bandwidth so we must make the low pass cutoff frequency W_{LP} as small as possible while still passing the first term in (96) or (97). Note also that since $\Delta\tau$ is much smaller than the reciprocal of the bandwidth of V_{c_1} or V_{s_1} we will have with $t' = t$ or $t' = t - \tau$

$$V_{c_1}(t' + \Delta\tau)V_{c_1}(t') + V_{s_1}(t' + \Delta\tau)V_{s_1}(t') \triangleq V_{c_1}^2(t') + V_{s_1}^2(t') \tag{98}$$

and

$$V_{c_1}(t' + \Delta\tau)V_{s_1}(t') - V_{c_1}(t')V_{s_1}(t' + \Delta\tau) \triangleq 0 \tag{99}$$

The final output, $v_{LP}(t)$, will have the form

$$v_{LP}(t) = K(t)\left[\langle V_{c_1}^2(t')\rangle + \langle V_{s_1}^2(t')\rangle\right]\cos(\Delta\phi \pm \omega_{IF}\tau_o) + n_o(t) \tag{100}$$

where $\langle\ \rangle$ indicates the passage of the enclosed term through the low pass filter. If this low pass filter were an ideal integrator these brackets would indicate time averaging. The term K(t) is a very slowly varying, almost constant, function whose origin lies in the antenna

amplitude function $\beta(t)$. The term $n_o(t)$ is a very small noise term residual that was passed through the low pass filter. Typical sample functions for the terms $K(t)$, $[\, V_{c_1}^2(t') + V_{s_1}^2(t') \,]$, and $n_o(t)$ are shown in Figure 20. For the sake of brevity we will denote the multiplicative term of the cosine function as $V_o(t)$.

$$V_o(t) \triangleq K(t)\left[\langle V_{c_1}^2(t')\rangle + \langle V_{s_1}^2(t')\rangle\right] \tag{101}$$

This term will, in general, be almost constant with a slight quasi-harmonic variation about the mean value $\langle V_o \rangle$ as shown in Figure 21. The minimum period of this quasi-harmonic variation will be limited by the low pass filter and will be approximately equal to the reciprocal of v_{LP}. The minimum value of W_{LP} will be set by the requirement that we must pass the cosine term shown in (96) or (97). The argument of this cosine term is the key to using the interferometer for navigation. To pass this cosine term the low pass filter must have an upper cutoff frequency of at least

$$W_{LP_{min}} \geq \frac{d}{dt}\left(\Delta\phi(t) \pm \omega_{IF}\tau_o(t)\right)\Big|_{max} \tag{102}$$

We will now define the local oscillator phase shift term $\phi_o(t)$ and show how the interferometer may be used for navigation. For a more comprehensive discussion of the correlation-receiver and other types of receivers the reader is referred to such references as Kraus, [3, pp. 236 - 290], Bracewell, [8], or Christiansen and Högbom, [9, pp. 190 - 210].

Figure 19 R.F., I.F., and Low-Pass Filter Transfer Functions

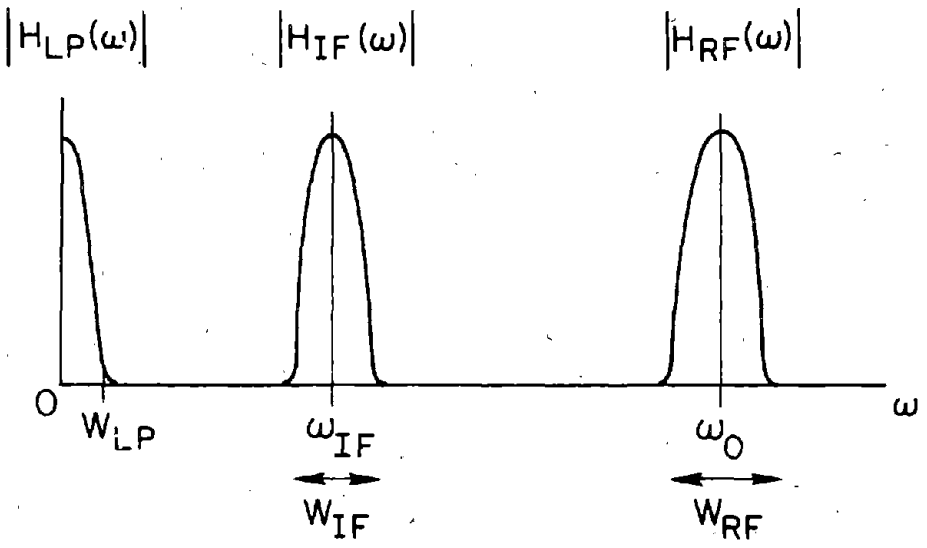

Figure 20 Sample Time Functions

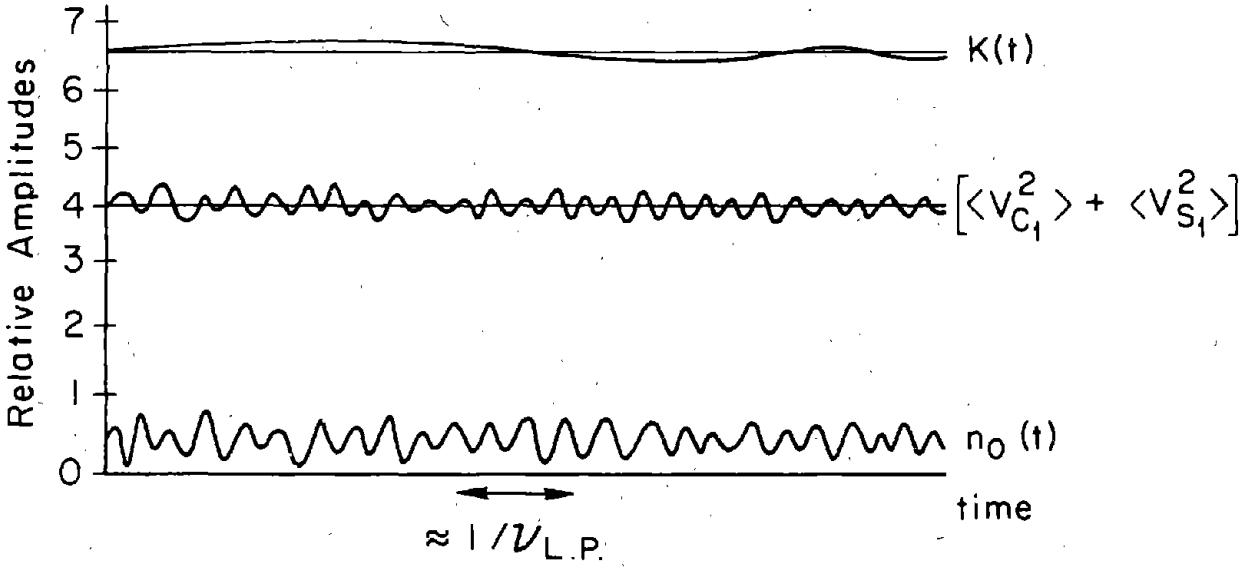

Figure 21 The Amplitude Multiplier of the Cosine Function

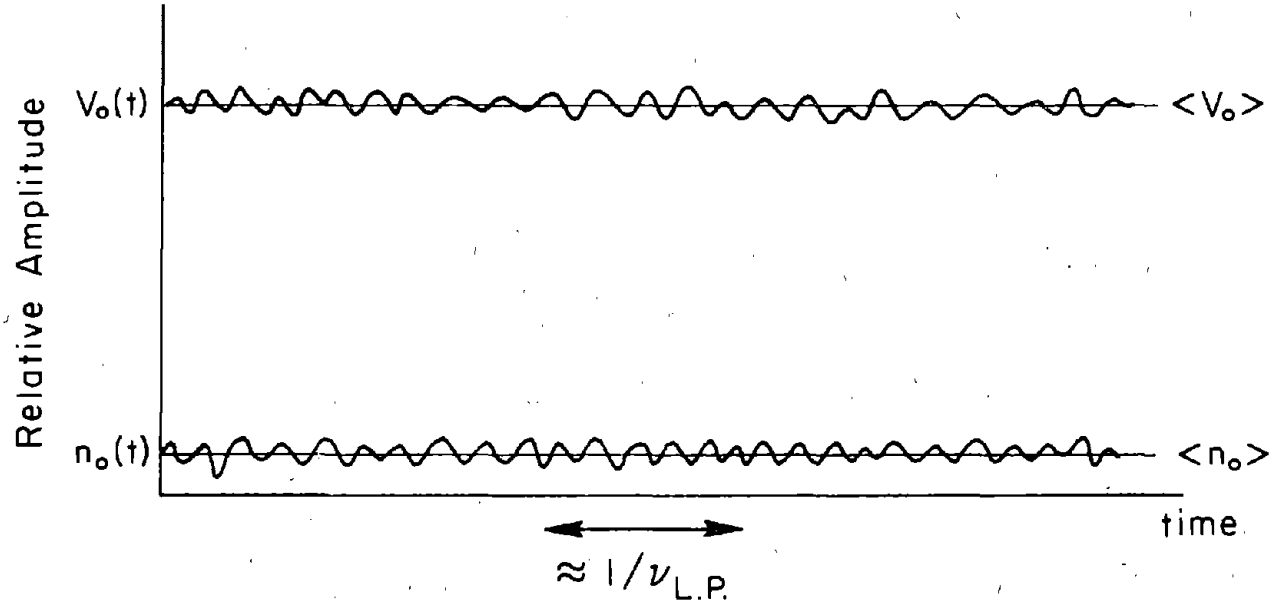

3.3 The Navigational Technique

All work up to this point was done to lay a foundation for this section. As was shown in the preceding section the output of the correlation receiver with the interferometer antennas tracking on a discrete source is given by

$$v_{LP}(t) = V_o(t) \cos \Delta\phi(t) \pm \omega_{IF}\tau_o(t) + n_o(t) \tag{103}$$

The phase difference term is given by

$$\Delta\phi(t) = \phi(t) - \phi_o(t) \tag{84}$$

where the term $\phi(t)$ is the unknown fringe phase of the source and $\phi_o(t)$ is the known phase injected into the local oscillator #2 as shown in Figure 18. The method to be presented in this section will, in principle, work for almost any $\phi_o(t)$ that is chosen. There is, however, an optimum choice for $\phi_o(t)$. Recall that in the last part of the previous section we discussed the minimum low pass filter cutoff frequency. Since the time-average noise power in $n_o(t)$ is directly proportional to W_{LP} we should make this cutoff frequency as small as possible while still passing the cosine term. The minimum cutoff frequency required to accomplish the passage of the cosine term is given in equation (102). It is apparent that a minimum W_{LP} will be allowed by minimizing $\Delta\phi(t)$ at all times. The optimum choice for $\phi_o(t)$ is thus the best guess we can come up with for $\phi(t)$. This best guess is obtained

directly from the antenna tracking procedures developed in section 2.5, as was also the best guess for $\tau_o(t)$ that was obtained in the previous section. If we obtain the best guess of $\hat{r}_{a_o}(t)$ in the "moving" coordinate system, (x_1, x_2, x_3), attached to the ship using equation (63)

$$\hat{r}_{a_o}(t) = \bar{\bar{T}}_2(t) \cdot \bar{\bar{T}}_1(t) \cdot \bar{\bar{R}}_o(t) \cdot \bar{\bar{A}}_o(t) \cdot \hat{r}(t), \tag{63}$$

where $\bar{\bar{T}}_1$, $\bar{\bar{T}}_2$, $\bar{\bar{R}}_o$ and $\bar{\bar{A}}_o$ are given using the procedures in section 2.5, the best guess for $\phi(t)$, namely $\phi_o(t)$, will be given by

$$\phi_o(t) = \frac{\omega_o n_s(t) S(t)}{c} \hat{r}_{a_o}(t)_{X_1} \tag{104}$$

This is, of course, just equal to $\omega_o \tau_o(t)$. The rationale behind the "best choice" for $\phi_o(t)$ can be summarized by stating that we wish to make the "frequency aperture" of the low pass filter as small as possible to restrict the passage of the noise term. At the same time we need to collapse the frequency spectrum of the phase term $\phi(t)$ so it will fit through the low pass frequency aperture. To accomplish this we subtract a best guess for $\phi(t)$, namely $\phi_o(t)$. Once the collapsed phase term passes through the low frequency aperture we add back the known term $\phi_o(t)$ and obtain $\phi_o(t)$ with a minimum noise transfer.

We will now discuss how we add back the term $\phi_o(t)$ onto the output phase. We will also subtract or add the known term $\omega_{IF}\tau_o(t)$ so we obtain the term $\phi(t)$ alone. The correlation receiver output, $v_{LP}(t)$ is sketched in Figure 22 including the noise term $n_o(t)$ and the amplitude term $V_o(t)$. Since the low pass filter is chosen to just pass the cosine term the periods

of variation of $V_o(t)$, $n_o(t)$ and cos $(\Delta\phi \pm \omega_{IF}\tau_o)$ will be about the same. The noise term $n_o(t)$ and the amplitude term $V_o(t)$ will inherently introduce slight errors in the measurement of the phase of the cosine term. The output, $v_{LP}(t)$, can be fed into a phase detector directly or can be prepared for phse detection using a shaping circuit. The phase detector can not detect the absolute phase of the cosine term but will give the relative changes of phase of the cosine term. There is thus an ambiguity of $2N\pi$ in the measured phase of $v_{LP}(t)$. This does not matter since we will only be interested in phase variations of $\phi(t)$. To obtain these phase variations of $\phi(t)$ we use the system shown in Figure 23. The input to the phase detector is the correlation-receiver's output, $v_{LP}(t)$, in analog form. The phase detector gives a digital output of the term

$$\Phi(t_K) = \Delta\phi(t_K) \pm \omega_{IF}\tau_o(t_K) + 2N\pi. \tag{105}$$

where $2N\pi$ is the unknown ambiguity in the absolute value and t_K are the discrete time values for which this function is read out. The resolution of t_K must be small enough to track the variation of $\Phi(t)$ closely. The measured numerical phase is then read into the adder circuit which adds the known $\phi_o(t_K)$ and $\pm\ \omega_{IF}\tau_o(t_K)$ to $\Phi(t_K)$. The numerical output of the adder will be $\phi(t_K) + 2N\pi$. Using this output we can obtain the change of phase of $\phi(t)$ between any two discrete times t_i and t_j by simple subtraction. Let us define this measured phase difference as

Figure 22 Correlation Receiver Output (Dashed lined indicates the output without noise and with a constant multiplier V_o)

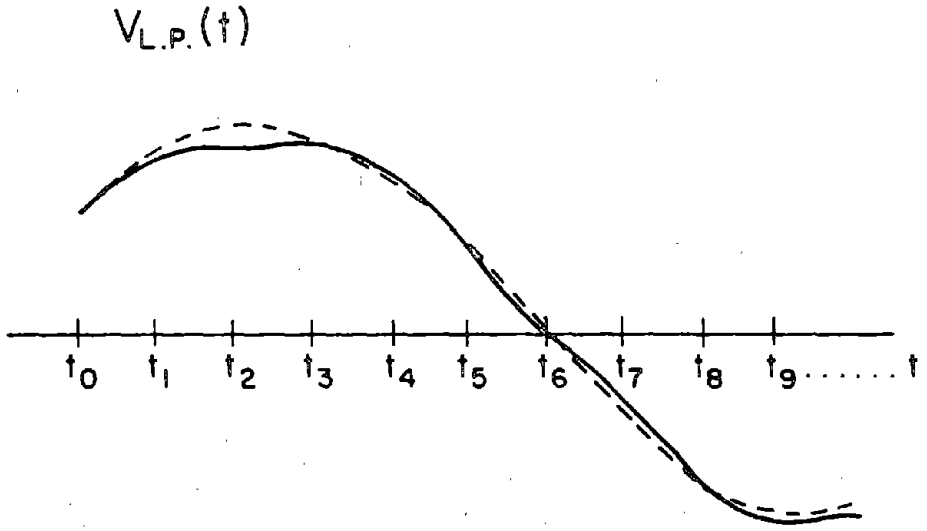

Figure 23 Fringe Phase Recovery System

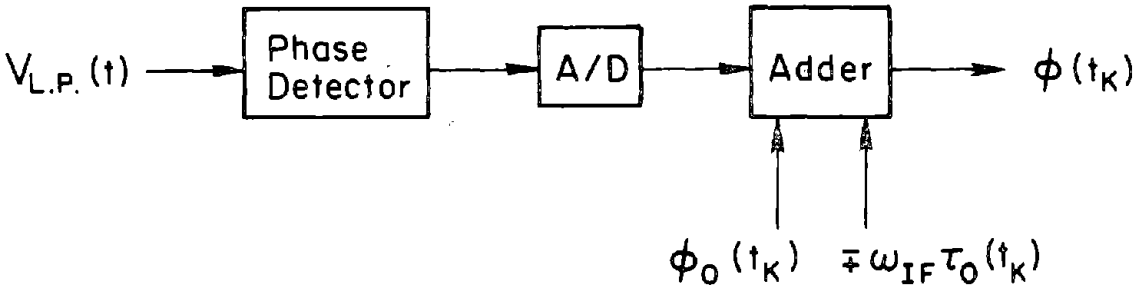

$$\gamma(t_i \mid t_j) \triangleq \phi(t_i) - \phi(t_j) \tag{106}$$

To see how we will use this measured phase variation to obtain the position of the ship we use (57) and (76) to write $\phi(t_i)$ as

$$\phi(t_i) = \frac{\omega_o}{c} n_s(t_i, \omega_o)\, s(t_i)\, \hat{s}'(t_i) \cdot \bar{\bar{R}}(t_i) \cdot \bar{\bar{A}}(t_i) \cdot \hat{r}(t_i) \tag{107}$$

Using (106) we obtain

$$\gamma(t_i \mid t_j) = \frac{\omega_o}{c} n_s(t_i) S(t_i) \hat{s}'(t_i) \cdot \bar{\bar{R}}(t_i) \cdot \bar{\bar{A}}(t_i) \cdot \hat{r}(t_i)$$

$$- n_s(t_j) S(t_j) \hat{s}'(t_j) \cdot \bar{\bar{R}}(t_j) \cdot \bar{\bar{A}}(t_j) \cdot \hat{r}(t_j) \tag{108}$$

A few approximations can be made for this expression. The first of these is the assumption that $n_s(t)$ is approximately constant over the course of several minutes. The second approximation will be to replace $\bar{\bar{R}}$ with the known matrix $\bar{\bar{R}}_o$. These approximations are made only to simplify the navigational technique and should introduce no serious errors. The success of the method is not contingent upon these assumptions and a more general, but messy, technique can easily be developed along the same lines as our simplified method, but without the above assumptions. Substituting the above assumptions into (108) we obtain

$$\gamma(t_i \mid t_j) = \frac{\omega_o n_s}{c} S(t_i) \hat{s}'(t_i) \cdot \bar{\bar{R}}_o(t_i) \cdot \bar{\bar{A}}(t_i) \cdot \hat{r}(t_i)$$

$$- S(t_j) \hat{s}'(t_j) \cdot \bar{\bar{R}}_o(t_j) \cdot \bar{\bar{A}}(t_j) \cdot \hat{r}(t_j) \tag{109}$$

When we look at this expression we notice that all terms on both the L.H.S. and R.H.S. of this equation are known or measured except $\overline{\overline{A}}(t_i)$ and $\overline{\overline{A}}(t_j)$. That is

a) $\gamma(t_i|t_j)$ is measured.

b) $S(t)$, the baseline length, is measured.

c) $\hat{s}(t)$, the unit baseline vector is measured in the horizon system. Its cartesian components are given in equations (11) to (13).

d) $\overline{\overline{R}}_o(t)$ is known using the technique of section 2.4.

e) $\hat{r}(t)$, the unit source direction vector in latitude-longitude coordinates, is known from tabulated data.

To simplify the notation to follow let us define the vector

$$\overline{B}(t) = \frac{\omega_o n_s}{c} \; S(t) \;\; \hat{s}'(t) \;\; \overline{\overline{R}}_o(t) \tag{110}$$

The components of this vector will be known. Substituting into (109) we obtain the equation

$$\overline{B}(t_i) \cdot \overline{\overline{A}}(t_i) \cdot \hat{r}(t_i) - \overline{B}(t_j) \cdot \overline{\overline{A}}(t_j) \cdot \hat{r}(t_j) = \gamma(t_i|t_j) \tag{111}$$

Using the 1,2,3 representation for the cartesian components of $\overline{B}$ and $\hat{r}$ we can rewrite equation (111) in the form

$$\sum_{m=1}^{3} \sum_{\ell=1}^{3} B_m(t_i)\, a_{m\ell}(t_i)\, r_\ell(t_i) - B_m(t_j)\, a_{m\ell}(t_j) r_\ell(t_j) = \gamma(t_i|t_j) \tag{112}$$

On examining $\overline{\overline{A}}(t)$ in equation (24) we notice that its unknown elements $a_{m\ell}(t)$, if found, would give us the position-longitude and latitude coordinates of the ship on the earth. Let us say we desire to know the

position of the ship at $t_j = t_o$. A knowledge of the matrix elements $a_{m\ell}(t_o)$ will provide us with the ship's position. We notice in equation (112) that there are two sets of unknowns, $a_{\ell m}(t_j) = a_{\ell m}(t_o)$ and $a_{\ell m}(t_i)$. To express $a_{\ell m}(t_i)$ in terms of the desired unknowns $a_{\ell m}(t_o)$, where $t_i \geq t_o$, we use the equations of evolution derived in section 2.2. Using these equations, (34) to (41), we substitute for $a_{\ell m}(t_i)$ in terms of $a_{\ell m}(t_o)$ in (112). The result can be expressed in the simplified form

$$\sum_{m=1}^{3} \sum_{\ell=1}^{3} F_{m\ell}\,(t_i | t_o)\;\; a_{m\ell}(t_o) \;=\; \gamma(t_i | t_o) \tag{113}$$

Where the coefficients $F_{m\ell}$ are given on the following page in terms of known or measured functions. The functions f_1, f_2, g, and g_2 are given in equations (29) to (32) and are measurable. Using (25), the matrix $\bar{\bar{A}}(t_o)$ is given by,

$$\bar{\bar{A}}(t_o) = \begin{bmatrix} \cos\lambda(t_o) & -\sin\lambda(t_o) & 0 \\ \sin\lambda(t_o)\sin\delta(t_o) & \cos\lambda(t_o)\sin\delta(t_o) & -\cos\delta(t_o) \\ \sin\lambda(t_o)\cos\delta(t_o) & \cos\lambda(t_o)\cos\delta(t_o) & \sin\delta(t_o) \end{bmatrix} \tag{114}$$

To obtain $f_1(t)$ and $f_2(t)$ from (29) and (30) we use the assumed value $\delta_o(t)$ for the declination $\delta(t)$.

The values of $F_{m\ell}$ are:

$$F_{11}(t_i|t_o) = B_1(t_i)\left[f_1(t_i)r_1(t_i) - f_2(t_i)r_2(t_i)\right] - B_1(t_o)r_1(t_o)$$

$$F_{12}(t_i|t_o) = B_1(t_i)\left[f_2(t_i)r_1(t_i) + f_1(t_i)r_2(t_i)\right] - B_1(t_o)r_2(t_o)$$

$$\begin{aligned}F_{21}(t_i|t_o) = {} & B_2(t_i)\left[f_1(t_i)g_1(t_i)r_1(t_i) - f_2(t_i)g_1(t_i)r_2(t_i)\right] \\ & + B_3(t_i)\left[f_1(t_i)g_2(t_i)r_1(t_i) - f_2(t_i)g_2(t_i)r_2(t_i)\right] \\ & - B_2(t_o)r_1(t_o)\end{aligned}$$

$$\begin{aligned}F_{22}(t_i|t_o) = {} & B_2(t_i)\left[f_2(t_i)g_1(t_i)r_1(t_i) + f_1(t_i)g_1(t_i)r_2(t_i)\right] \\ & + B_3(t_i)\left[f_2(t_i)g_2(t_i)r_1(t_i) + f_1(t_i)g_2(t_i)r_2(t_i)\right] \\ & - B_2(t_o)r_2(t_o)\end{aligned}$$

$$F_{23}(t_i|t_o) = B_2(t_i)\left[g_1(t_i)r_3(t_i) + g_2(t_i)r_3(t_i)\right] - B_2(t_o)r_3(t_o)$$

$$\begin{aligned}F_{31}(t_i|t_o) = {} & B_2(t_i)\left[f_1(t_i)g_2(t_i)r_1(t_i) + f_2(t_i)g_2(t_i)r_2(t_i)\right] \\ & + B_3(t_i)\left[f_1(t_i)g_1(t_i)r_1(t_i) + f_2(t_i)g_1(t_i)r_2(t_i)\right] \\ & - B_3(t_o)r_1(t_o)\end{aligned}$$

$$\begin{aligned}F_{32}(t_i|t_o) = {} & -B_2(t_i)\left[f_2(t_i)g_2(t_i)r_1(t_i) + f_1(t_i)g_2(t_i)r_2(t_i)\right] \\ & + B_3(t_i)\left[f_2(t_i)g_1(t_i)r_1(t_i) + f_1(t_i)g_1(t_i)r_2(t_i)\right] \\ & - B_3(t_o)r_2(t_o)\end{aligned}$$

$$F_{33}(t_i|t_o) = r_3(t_i)\left[B_3(t_i)g_1(t_i) - B_2(t_i)g_2(t_i)\right] - B_3(t_o)r_3(t_o)$$

(115)

There are several algebraic techniques for extracting the position coordinates $\lambda(t_o)$ and $\delta(t_o)$ from the set of equations in (113). All of these techniques, but one, require the solution of a nonlinear and mixed system of equations. Looking at (114) we see that there are only two "independent" variables, $\lambda(t_o)$ and $\delta(t_o)$, that generate the eight nonzero elements of the $\overline{\overline{A}}$ matrix. These independent variables generate the matrix elements in a nonlinear manner through transcendental equations. Even though there are only two "independent" variables $\lambda(t_o)$ and $\delta(t_o)$ the equation (114) can generate eight "linearly independent" equations in the eight linearly independent variables $a_{m\ell}(t_o)$ (with $a_{13} = 0$). As an example of the linearization of a nonlinear system consider the equation

$$\sin \chi_o + y\ (t) \cos \chi_o = Z(t) \tag{116}$$

This is a nonlinear transcendental equation in the single unknown χ_o. If we let $W_o = \sin \chi_o$ then this becomes a nonlinear equation in W_o.

$$W_o + y(t)\sqrt{1 - W_o^2} = Z(t) \tag{117}$$

The functions y(t) and Z(t) are parametric in the variable t. They are not independent but can assume different but coupled values as t is changed. The system (one equation) in (117) can be solved for W_o directly using only one value of t. We can, however, also solve the system by defining a second linearly independent variable $W_1 = \cos\chi_o$

and rewriting (116) as

$$W_o + y(t)\, W_1 = Z(t) \tag{118}$$

If we let t take on the values t_a and t_b we obtain the coupled system of two linearly independent equations

$$\begin{aligned} W_o + y(t_a)\, W_1 &= Z(t_a) \\ W_o + y(t_b)\, W_1 &= Z(t_b) \end{aligned} \tag{119}$$

which can be solved directly by elimination.

In the same manner as we converted the nonlinear equation in (116) to the linear system in (119) we will now convert the nonlinear system in the two variables, $\lambda(t_o)$ and $\delta(t_o)$, in (113) to a higher order system in the eight linearly independent variables $a_{m\ell}(t_o)$. Thus, the technique for obtaining the ship's position at any time, t_o, is to measure and calculate the values $F_{m\ell}(t_i\, t_o)$ and $\gamma(t_i\, t_o)$ for eight consecutive discrete times $t_i > t_o$. We then simply solve the linear system of eight equations in eight unknowns.

$$\sum_{m=1}^{3} \sum_{\ell=1}^{3} F_{m\ell}(t_i | t_o)\, a_{m\ell}(t_o) = \gamma(t_i | t_o) \qquad i = 1,8 \tag{120}$$

We need only to solve this linear system for two unknowns such as

$$a_{11}(t_o) = \cos\lambda(t_o) \tag{121}$$

and

$$a_{33}(t_o) = \sin\delta(t_o) \tag{122}$$

to obtain the ship's position at any time, t_o. This solution can be obtained easily using numerical methods such as Gauss' elimination or even a direct use of Cramer's rule. Note that our solution for position will be at a previous time, t_o. To obtain the position measurement at a future time we obtain

$$a_{12}(t_o) = -\sqrt{1 - a_{11}^2\ (t_o)} \tag{123}$$

and

$$a_{23}(t_o) = -\sqrt{1 - a_{38}^2\ (t_o)} \tag{124}$$

then directly use the equations of evolution in (35) and (42)

$$\cos \lambda(t) = f_1(t)\ a_{11}(t_o) + f_2(t)\ a_{12}(t_o) \tag{125}$$

$$\sin \delta(t) = g_1(t)\ a_{33}(t_o) + g_2(t)\ a_{23}(t_o) \tag{126}$$

In the preceding sections we used the term "assumed (or known)" ship position, unit direction vector, etc. The technique involved here is a convergent one in that after we start up the system by "assuming" a position so we can point the antennas and begin reading data, the data we obtain will yield position measurements that are superior to our initial assumption. Once the system is started up it should operate continuously even in moderately heavy seastates. In this way our "assumed" position will be based on past measurements and the use of the equations of evolution; and the position should be very accurate.

There are six sources of measurement error in this formulation whose effects will have to be considered in more detail in a future study in order to make a final evaluation of the realizable accuracy of the interferometer-navigational system. These sources of error, not necessarily in order of dominance, are

a) The effect of the noise term $n_o(t)$ on the phase measurement of the cosine term.

b) The accuracy of the ship motion measurements using the accelerometer technique described in section 2.1.

c) The accuracy of the bearing angle measurement, $\gamma_o(t)$. (In this worker's opinion this measurement may be the dominant source of error in the entire technique).

d) The error induced by assuming a spherically symmetric stratified index of refraction in developing the refraction matrix approximation in section 2.3 and in developing the time-varying phase path difference formulation in section 3.1.

e) The error in measuring the surface refractivity $N_s(t,\omega_o)$ and index of refraction $n_s(t,\omega_o)$ used in the refraction matrix approximation and time-varying phase path difference formulation.

f) The accuracy of the ship velocity measurement used in f_1, f_2, g_1 and g_2 given in equations (29) to (32).

IV. REFERENCES

[1] S. Blagoreshchenskii, Theory of Ship Motions, Volumes I and II, Dover, New York, 1962.

[2] J. Beurs, Speed and Pitching, Kemperman, Haarlem, 1957.

[3] J. D. Kraus, Radio Astronomy, McGraw-Hill, New York, 1966.

[4] A. Sommerfeld, Optics, Academic Press, New York, 1964.

[5] B. Bean and E. Dutton, Radio Meteorology, Dover, New York, 1968.

[6] R. E. Collin, Foundations for Microwave Engineering, McGraw Hill, New York, 1966.

[7] D. J. Sakrison, Communication Theory, Wiley, New York, 1968.

[8] R. N. Bracewell, "Radio Astronomy Techniques", Handbuch der Physik, vol. 54, pp. 42 - 129, Springer-Verlag OHG, Berlin, 1962.